ASM Handbook, Volume 22B, *Metals Process Simulation*
D.U. Furrer and S.L. Semiatin, editors

Modeling of Residual Stress and Machining Distortion in Aerospace Components

Kong Ma and Robert Goetz, Rolls-Royce
Shesh K. Srivatsa, GE Aviation

THE INSERTION OF NEW MATERIALS into aircraft systems takes several years and many millions of dollars. Experimental trials to define the manufacturing process to meet the specifications can add significant time and cost. Many military programs have small lot production in either initial engine development programs or specialized production, providing additional criticality to improving the first-time yield of manufacturing processes and quickly resolving production issues. Additionally, the impact of an unintended process change is unknown without evaluating the component, again adding time and cost to issue resolution. Therefore, new approaches are required to facilitate the rapid certification of materials and processes technologies. Significant improvements in manufacturing processes have been realized by process modeling tools such as DEFORM (Scientific Forming Technologies Corp.) and FORGE (Transvalor) for metal forming and ProCAST (ESI Group) for casting, which are now in routine industrial use. Modeling and simulation are critical for increasing the affordability of current and future aerospace materials and products and in developing and certifying materials in a shorter timeframe that more closely matches the product design cycle.

Introduction—Residual Stress, Distortion, and Modeling

Technical Need

Aircraft engine and airframe structural components that are machined from forgings or plate stock represent a significant cost for both military and commercial aircraft. Typical component applications, as shown in Fig. 1, are rotating disks in aircraft engines and structural components in airframes. The buy-to-fly weight ratio, which is the ratio of the forged material weight to the finished component weight, is typically between 4 and 10 for such components. The excess material is removed by various machining operations, which are a major contributor to the cost of forged components.

Metallic components undergo various forming processes, such as casting, forging, rolling, and so on, in which the material is heated to high temperatures. A typical wrought component of a titanium- or nickel-base alloy begins as an ingot. The cast structure is broken down into billet form, which is then forged into the rough shape of the component, with positive stock surrounding the finished shape. Deformation occurring during the forming process causes residual stresses that can be compounded by thermal gradients. After forming, the components are subjected to a series of heat treatment processes to improve the microstructure and material properties (e.g., toughness, strength, creep, fatigue). Most heat treatment processes involve heating the material to a high temperature to produce a change in microstructure (e.g., phase transformation, recrystallization).

Nickel-base superalloy disks used in aircraft engines typically undergo a two-step heat treatment process: solutionizing and aging. The first step is a solution heat treatment, and the solution temperatures are often high enough (~1100 °C, or 2000 °F, depending on the alloy) to almost completely relax any preexisting residual stress induced during the forming process. When the components are removed from the heat treat furnace at the end of the heating and soaking process, they are transported to the quenching station, during which the components lose heat to the ambient atmosphere due to radiation to the surrounding surfaces, natural convection through air, and conduction to the handling mechanism through the direct contact areas. This period is called the quench delay or transfer time and usually is very short (15 to 60 s).

This period is followed by rapid quenching. When the component is subjected to the much cooler quench medium (typically oil, water, polymer, salt, or forced air), the outer surface of the component cools down rapidly, contracts, and metallurgically stabilizes when it reaches a relatively low temperature (e.g., below 480 °C, or 900 °F, for nickel alloys), while the interior is still at a high temperature. At this point, the outside of the component is under tensile stress and yields, while the interior material is under compression because the outer volume cannot contract (inward) against the yet-to-contract hot interior. Gradually, the heat from the inside dissipates outward. The interior material then tries to contract, but now the outer volume is already relatively fixed because it is at a much

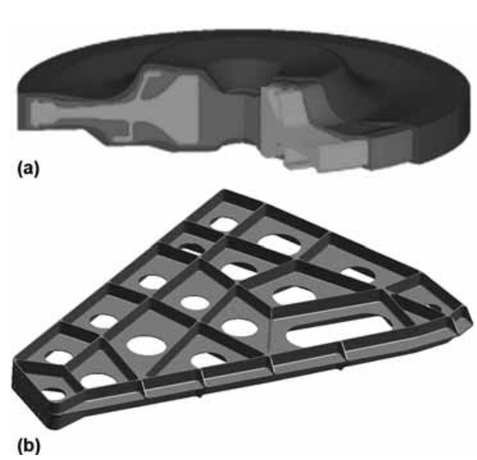

Fig. 1 Aircraft engine and airframe components with large buy-to-fly ratios and high machining costs. (a) Typical aircraft engine forging. Blue (dark outer region): forging shape; red (central region): intermediate shape; green (bright core region): finish machined shape; large volume of material machined away. (b) Typical airframe structural forging. Intricate geometrical features result in a large volume of material being machined away

lower temperature. Therefore, the interior is under tension and the outer region is under compression, because it is being pulled inward by the inner material. Plastic deformation subsequent to yielding induces bulk residual stresses in all directions.

Temperature gradients during quenching cause thermal stresses, which drive localized plastic deformation and residual stress buildup. Upon cooling to room temperature, residual stresses can exceed half of the alloy tensile strength. Often, to obtain favorable material strength and microstructure, fast cooling (quenching) is applied. Higher cooling rates result in higher residual stresses. Residual stresses resulting from thermomechanical processing can cause in-process cracking, machining distortion, in-service distortion, and/or lowered life.

The stress profile within a component depends on the local geometry features and the temperature difference between the near surface area and the quench medium (which determines the rate of heat loss). An area with a thinner cross section usually has lower stress than an area with a thicker section. Variations in residual stress occur due to variability in manufacturing process conditions, for example, the loading pattern of components in the furnace and quench medium, the agitation level in quench tanks, and the nature of the heat treat fixtures.

During the second heat treatment step, known as aging, the component is reheated to a temperature much lower than the solution temperature (typically 650 to 820 °C, or 1200 to 1500 °F) to form secondary and tertiary gamma prime in nickel-base superalloys. This step completes the transformation to the desired microstructure and properties, with the added benefit of stress relaxation through creep and recovery processes. The amount of stress relaxation depends on the time and temperature of the age cycle and the magnitude of the initial residual stress. Higher temperatures result in a greater degree of relaxation. Stress relaxation is related to the creep behavior of the material, and therefore, the microstructure (grain size and gamma prime) also affects stress relaxation. If the level of residual stress is below the steady-state relaxation stress, further relaxation will not occur unless higher temperatures are used. Thus, residual stress cannot be eliminated, only reduced during final aging, and the component still has enough residual stress to affect its behavior during machining and in service.

Component distortion can be caused by material bulk stresses resulting from heat treating operations and/or by local near-surface machining-induced stresses. When the component cross section is thick, bulk residual stresses dictate component distortion. As the cross section is machined thinner (~3 mm, or 0.125 in.), surface residual stress begins to play a more significant role in component distortion.

The prediction of residual stresses at quantified levels of uncertainty can improve processing methods, component design, robustness, performance, and quality as well as achieve more efficient material utilization and aircraft system efficiency, which result in lower environmental impact. Distortion of machined titanium and nickel alloys contributes significantly to the cost of these components. Heat treatment and machining are the two critical operations in the manufacture of engine and airframe components that influence residual stress. Residual stresses and associated distortion have a significant effect on manufacturing cost in four distinct ways.

First, the forging and intermediate heat treat shapes contain additional material to account for expected distortion (Fig. 2). This material, added to ensure a positive material envelope over the finished component shape, represents a raw material cost and increases the machining cost. This additional material also imposes a limit on the benefit of near-net shape forging, which is being vigorously pursued by the industry.

Second, component distortion during machining requires that the machining process engineer plan machining operations and fixtures so that distortion does not compromise the finished component shape. Distortion during and after machining can result in added operations, such as lineup and straightening, rework, or scrap. Typically, additional machining operations and setups are added in a time-consuming and costly trial-and-error approach to minimize the effects of component distortion. For example, components such as disks are machined alternately on either side in an attempt to stepwise balance the distortion. The time spent "flipping" components erodes productivity for thick, stiff components; for thin components, the strategy may be inadequate.

Third, residual stresses and associated distortion add complexity to machining process development and shop operations. Distortion affects the details of the machining plan and the way the component interfaces with machining fixtures. These effects generally vary between material suppliers, from lot to lot, and from one machining process to another. Distortion thereby not only influences the effort incurred during initial development of machining plans but may require adjustments after the initial plan has been set.

Finally, distortion results in preload of aircraft structures and fasteners and can cause assembly problems. Manufacturing residual stresses can adversely impact the behavior of the components during service. Distorted and prestressed components can result in fatigue capability degradation by increasing the local mean stresses. Residual stresses affect the dimensional stability of rotating components in aircraft engines. These components are exposed to high temperatures for long times, and distortions can affect system tolerances, clearances, and efficiency. For an accurate analysis of component behavior during service, the manufacturing residual stresses must be included as initial conditions.

The physics and mathematics of residual-stress redistribution within a component during machining are well understood. Determining residual stresses and subsequent distortion requires modeling using finite-element methods. This method has been used to evaluate the effect of processing conditions on residual-stress development and the effect of residual stresses on distortion during machining. The buildup of residual stresses during heat treatment and machining are difficult to assess using intuition, engineering judgment, or empirical methods. The physical interplay of quench heat transfer, elevated-temperature mechanical behavior, and localized plastic deformation is complex. Subtle changes in processing conditions and component geometry can significantly affect the magnitude and pattern of residual stresses.

For routine use, a fast-acting, validated, physics-based model with sufficient fidelity and robustness is needed to accurately predict the effects of thermomechanical processing and reduce scatter in residual stress, microstructure, mechanical properties, and their measurement. Residual-stress modeling technology must be standardized to meet an industry requirement for accuracy and capability in manufacturing (distortions), service (dimensional stability), service-life estimation (fatigue life, crack initiation, crack growth and propagation), and material testing (measurement scatter and sampling effects).

There is a need to understand the effects of heat treating and machining on distortion and

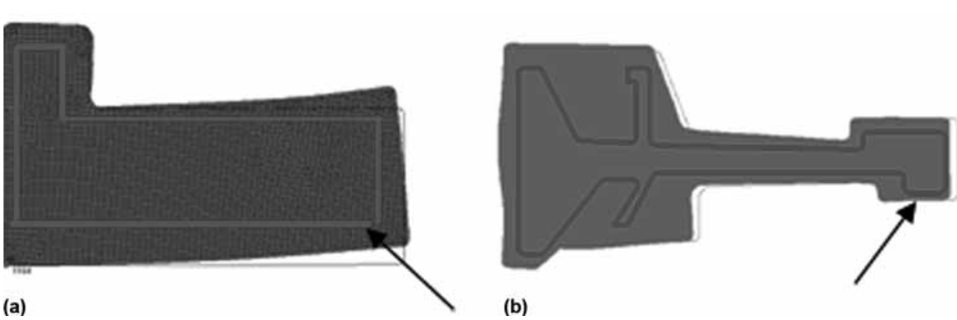

Fig. 2 Extra material envelope is needed to compensate for distortions during heat treating and machining to the inside finished component shape

to predict, minimize, and control these distortion-related processes to achieve robust six-sigma quality. There is a need to develop heat treatment and machining processes for minimizing distortions, realizing that this is not always the same as minimizing residual stresses. In addition, there is a need to accurately predict residual stress and consider its impact on component life and behavior in service. The industrial drive is toward stronger and longer-lasting components with higher-temperature capability. As new materials with better properties to meet more exacting requirements are introduced, they will be more difficult to machine. While materials scientists are developing higher-temperature materials, it is also possible to further improve existing designs and materials. One way to improve component design and increase life is by understanding the distribution of residual stress from the manufacturing process and linking it with the product life cycle. Modeling will help reduce machining problems and thereby enable more rapid introduction of high-performance materials and components.

Objectives of Residual Stress and Machining Distortion Modeling

The overall objective is to develop and validate a high-productivity modeling method that accurately predicts the magnitude and pattern of distortion during machining of forgings used in aircraft engines and airframe structures and to establish an approach for using machining modeling to generate machining plans that yield less component distortion and reduce the cost of machining.

Metals Affordability Initiative Programs

For almost a decade, the United States Air Force (USAF) Metals Affordability Initiative (MAI) has devoted significant resources to understanding the impact of residual stresses on component variability and machining distortion. The MAI team consists of materials developers, forgers, software developers, universities, aircraft engine makers, and airframers to bring the real-world perspectives of the entire supply chain to the project. The methods developed represent a sound engineering practice for predicting machining distortion and are available for licensing in commercial codes. Many aerospace original equipment manufacturers and their suppliers now have established in-house analysis methods. The MAI projects have reduced the time to implementation of the process technology by permitting a focused, larger-scale, complete effort across engine manufacturers, airframers, and material and machining suppliers than would be possible if efforts were conducted by individual companies alone.

Significant progress was made in the development and validation of two-dimensional (2-D) modeling tools for predicting machining distortions in the USAF MAI Dual-Use Science and Technology (DUST-7) Program, Cooperative Agreement F33615-99-2-5216. This program advanced the state of the art in going from the previous state of a time-consuming, manual, partially validated, not-production-ready procedure to an automated, high-productivity, user-friendly, fast-acting, validated, commercially supported, and production-ready analysis tool that can be used to achieve significant cost-savings. It was shown that 2-D distortions can be predicted to within the typical process variability of $\pm$20 % or $\pm$5 mils (0.125 mm).

Aircraft engine rotating components are 2-D axisymmetric up until the final machining operations, when three-dimensional (3-D) features such as dovetail slots, cooling holes, and so on are machined. For this reason and because of the simpler nature of 2-D models as compared to 3-D, the development of 2-D tools was addressed first. The 2-D model was rigorously validated first on simple-shaped forgings and later for complex shapes in a production environment. Two-dimensional rotating disks account for the majority of aircraft engine forgings. The machining model developed realistically captures the process boundary conditions (tooling constraints) for any user-specified sequence of machining operations. The method was rigorously validated first on simple shapes in a well-controlled situation and then extended to complex shapes in a production environment. The material chosen for this program was cast and wrought U720, but the model/method is pervasive and can be employed for other materials.

The 2-D model has been implemented at various aircraft engine makers, and it has been used successfully for many production components. This analytical tool guides machining operation sequence and tooling design for rotor hardware to minimize component distortion, which was previously predominately an experience-based trial-and-error process.

Following the successful completion of the 2-D program, the MAI team has developed 3-D distortion modeling tools. The results presented in this article are largely based on the MAI programs.

Modeling of Heat-Treat-Induced Residual Stress

Finite-Element Residual-Stress Analysis

Residual-stress analysis involves:

- Determination of heat-transfer coefficients during quenching
- Measurement of material constitutive behavior (elastic-plastic creep) at processing conditions
- Finite-element analysis to calculate thermal and stress fields
- Finite-element analysis for machining distortion
- Finite-element analysis for in-service distortion and for strength and service-life estimation

Commercially available process modeling tools, such as DEFORM and FORGE, are finite-element-based analysis tools. They employ an elastic-plastic formulation, which is the necessary basis for the model formulation. The detailed steps of setting up a model for the heat treatment process vary depending on the software used. However, they all involve several general steps:

1. Construct the heat treat geometrical model from computer-aided design (CAD) tools.
2. Obtain the thermophysical material properties for the component material. This includes thermal conductivity, heat capacity, density, thermal expansion coefficient, Young's modulus, and flow stress describing plastic behavior. All properties are temperature dependent and also depend on the microstructure and previous processing history of the material. The use of realistic material data is critical to the success of any modeling effort.
3. Obtain the detailed process information. This includes the heat treat solution temperature, soak time, quench delay time, quench medium type, medium temperature, component loading configuration, and so on. Similar processing data are needed for any subsequent stress relief (or aging) processes.
4. Determine the heat-transfer coefficients (HTCs) for the interface between the quenching medium and the component. Using the analytical approach, one can use the sophisticated two-phase (gaseous and liquid) flow computational fluid dynamic methods to simulate the quenching agitation interacting with the specific component geometry. This requires very detailed characterization of the physical quenching configuration and is time-consuming. A much simpler approach is to experimentally determine the effective HTCs by instrumenting an experimental component with thermocouples. The HTCs are then input into the modeling software as time- and temperature-dependent boundary conditions.
5. Mesh the component geometry. All the general rules and guidelines used for standard finite-element analysis apply to the process model; for example, quad elements are better than triangular elements, a higher-density mesh yields more accurate results, and so on. One point worth noting is that the elastic-plastic formulation is used to perform the thermomechanical analysis of components. Therefore, particular attention should be given to the mesh density in the areas subjected to steep thermal and mechanical changes during the heat treat cycle.
6. Run the heat treat model. Because of the complexity of the algorithm and the time and temperature base of the process model, it usually takes from a few hours for a

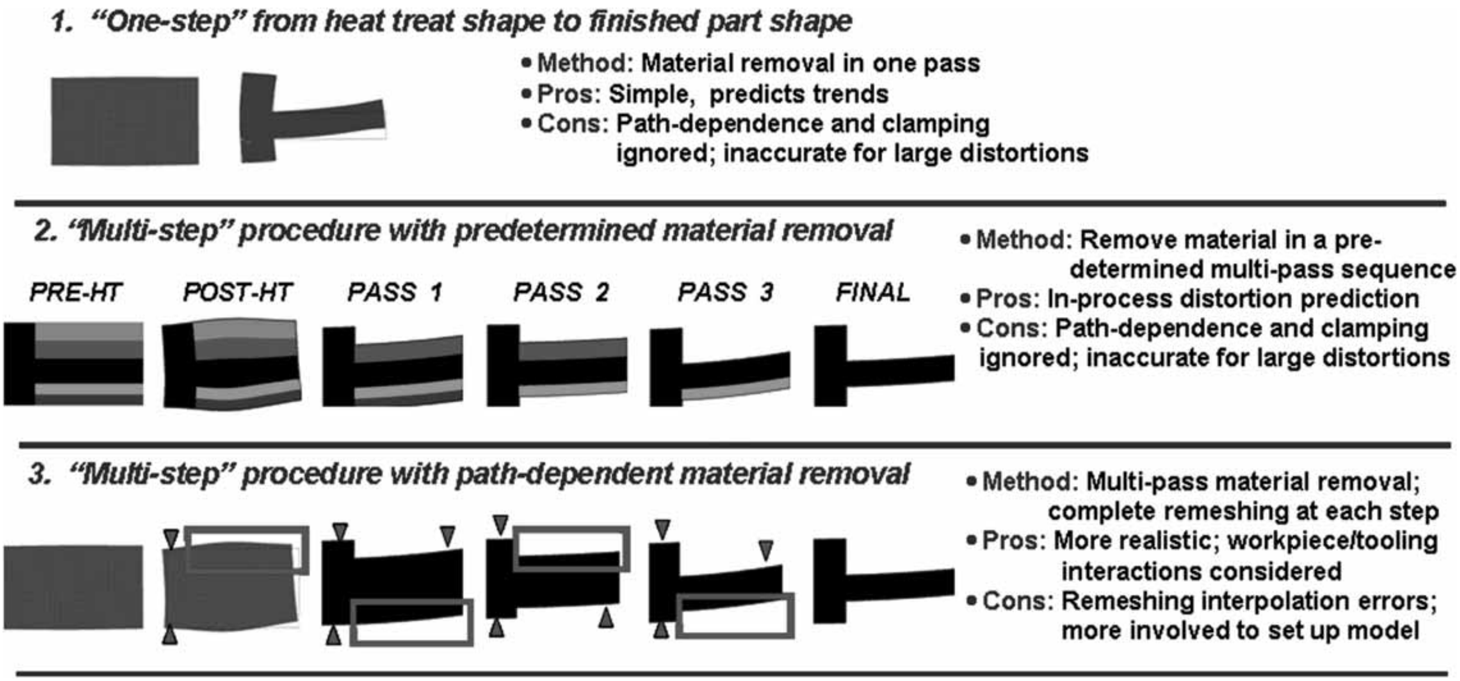

Fig. 3 Comparison of various machining distortion prediction methods. The multistep procedure with path-dependent material removal most accurately represents what is happening in practice

mid-sized 2-D model to several days for a complex 3-D model. Like any finite-element analysis, if the solution fails to converge, the use of smaller simulation time-steps and/or altering the mesh can help eliminate the problem.

Modeling Procedures (2-D)

Generally, three procedures have been commonly used to model the machining distortion (Fig. 3). All of these techniques use different methods for how the material is removed during machining and the subsequent re-equilibration of residual stresses. All of the techniques described as follows neglect the surface residual stress induced by the interaction between the machine tool and the component, and therefore, the effect of cutting conditions is also ignored. The effect of machining-induced stresses is addressed in a later section in this article.

Method 1. In the one-step procedure, plastic strains from the heat treat shape are mapped onto the machined shape, and the strains and stresses are re-equilibrated to obtain the resulting distortion. In essence, this method means that all the material is machined off instantaneously in one machining pass. This method is straightforward and easy to implement; it avoids remeshing associated with modeling each machining operation, and it predicts bulk distortions and trends correctly. However, it ignores the influence of the machining path and the effect of in-process shape change on the workpiece/fixture interface, and its accuracy decreases with increasing distortion.

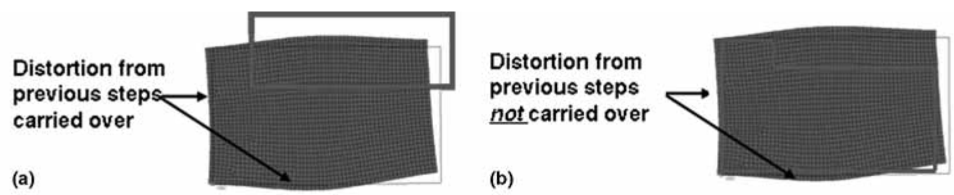

Fig. 4 (a) Boolean and (b) remeshing procedures

Method 2. The multistep procedure with predetermined material removal is similar to the one-step procedure, but material is removed in multiple passes based on a predetermined machining sequence. The workpiece is meshed up front to follow the machining sequence. This method also avoids remeshing associated with modeling each machining operation, and it predicts bulk distortions and trends correctly. However, it ignores the influence of the machining path and the effect of in-process shape change on the workpiece/fixture interface, and its accuracy decreases with increasing distortion. The initial meshing is more involved than the one-step method. If changes in machining sequences are to be evaluated, the heat treat analysis must be completely redone.

Method 3. In the multistep procedure with path-dependent material removal, a complete remeshing is performed at each machining operation, and the material removal follows the actual machining sequences. This is a more realistic representation of the machining process, and it accounts for in-process distortions and workpiece/tooling interactions. It is most involved to set up the model. The material removal can be accomplished in two ways: Boolean or remeshing.

Boolean Procedure. The material inside the machining path is removed to obtain the new geometry by a Boolean operation of the current geometry and the machining path (Fig. 4a). The new geometry follows the distorted geometry from the preceding step everywhere except where the machining cut is taken. This new geometry, which represents the workpiece shape after machining, is remeshed and the stresses/strains re-equilibrated to obtain the unrestrained distortion. When the Boolean cut is very thin (e.g., on the last pass) and the workpiece is not constrained during cutting, there will be very little additional distortion, and the cut face will follow the cutting tool path.

Remeshing Procedure. The plastic strains from the current geometry are mapped onto the machined geometry and the stresses re-equilibrated to obtain the resulting distortion. The new geometry follows what the user has predefined and not the distorted geometry from the previous step. The new geometry is indicated by the solid line. Remeshing to this new

Fig. 5 Distorted airframe component. This component was machined flat. The material stress and machining-induced stress are causing it to distort

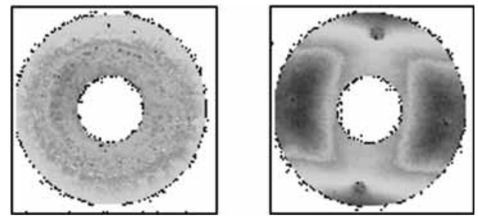

Fig. 6 Optical scan pictures showing axisymmetric and nonaxisymmetric distortion (due to nonaxisymmetric fixturing) following heat treatment. Colors indicate axial distortion.

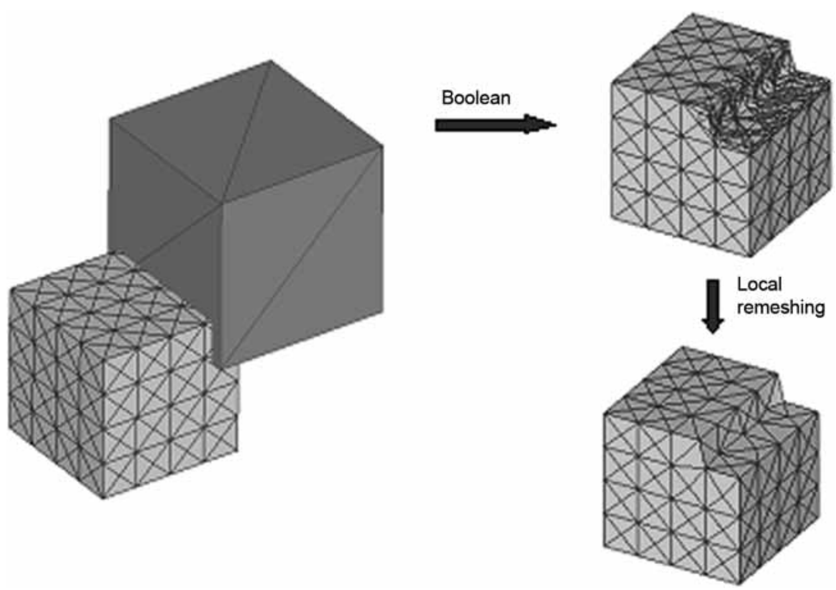

Fig. 7 Local remeshing of elements affected by the machining process

geometry causes the distortion from the preceding steps not to be carried through, as shown on the uncut faces in Fig. 4(b).

Of the three methods shown in Fig. 3, method 1 is straightforward, and methods 2 and 3 require a large amount of user time to set up the problem for a general multistep machining process. As a result, such analyses are not performed routinely. An automated version of method 3 that minimizes model set-up time, streamlines the overall procedure, and minimizes the interpolation error was developed in the MAI programs.

Modeling Procedures (3-D)

Three-dimensional distortion modeling is needed to address airframe structures and complex engine components. Figure 5 shows a distorted airframe component with a 3-D geometry. Figure 6 shows both axisymmetric and nonaxisymmetric distortions of a nominally 2-D axisymmetric-shaped engine disk forging.

In the modeling of the material-removal process during machining, a new finite-element mesh must be generated on the as-machined shape. Residual stresses and strains must be interpolated from the premachined shape (mesh) to the postmachined shape (mesh). This process of interpolation introduces errors in the simulation that can be significant if the component geometry has thin walls adjacent to thicker sections. This problem is more acute in 3-D modeling than in 2-D modeling because of the increased geometrical complexity of 3-D shapes (thin/thick sections) and because of the limitations on the fineness of the mesh that can be employed in 3-D to keep the computations manageable. The solution accuracy was improved with a combination of controlling the local mesh density to have finer elements in thin geometrical features and high-stress gradient regions, local remeshing, and improved interpolation schemes.

Local Remeshing. During global remeshing, a completely new mesh is generated over the entire volume of the workpiece. Therefore, every element and node in the model is changed, and the state variables are interpolated from the old mesh to the new mesh. This introduces large interpolation errors. During material removal, generally only a small volume of the workpiece geometry is altered. Figure 7 shows a schematic of the material-removal process. In the local remeshing methodology, only the elements along the machined surface and their neighboring elements are remeshed. As compared with the original mesh, 86.7% nodes and 79.6% elements remain unchanged in this example. During data interpolation, only the modified nodes/elements are affected. Therefore, interpolation error can be avoided for the major part of the mesh that remains unchanged.

Improved Interpolation. Two new interpolation schemes were developed. In the first, the interpolation is performed based on a local polynomial fit. In the second, the element variables are also stored at the nodes and the nodal values used during interpolation, which avoids the error during transfer of element data to nodes. The interpolation error was reduced significantly with the new interpolation schemes. When interpolating onto the same mesh, the error in radial distortion was reduced to 2.5% as compared to 50% with the old method.

The method of combining local remeshing, improved interpolation, and mesh windows to control element size helps reduce errors. In general, this method results in peak values of stress and strain being retained more accurately than the previous methods; that is, there is less smoothing error with the new method. Simulation results were found to be in good agreement with experimental data. All predictions were within 20% of the measurements with the new method.

To easily set up the model for multiple machining operations and passes, a template (Fig. 8) was set up that can position the workpiece, the fixtures and loads, and the material removal in a user-friendly setup. A preview of all the machining steps ensures error-free setup before the simulations are commenced.

To facilitate the material-removal process for machining distortion modeling, the machining path information (described by G-code) was converted to a geometry that can be used to generate the machined workpiece configuration (Fig. 9). A G-code interpreter was developed and tested with several examples (Fig. 10).

During the simulation of residual stresses and machining distortions, it is necessary to constrain the six degrees of freedom in the workpiece to eliminate rigid body motion. Guidelines were developed on the selection of the nodes and the manner in which they must be constrained. A preprocessing function was developed to automate/guide the definition of these boundary conditions. The method is:

1. Fix one node in x-, y-, z-directions. This removes the three degrees of freedom in translation.
2. Find a point at the same x and z but different y. Fix this in the z-direction; it removes x-rotation.
3. Find a point at the same y and x but different z. Fix this in the x-direction; it removes y-rotation.
4. Find a point at the same z and y but different x. Fix this in the y-direction; it removes z-rotation.

The machining distortion solution is dependent on the chosen reference boundary conditions to constrain rigid body motion. A facility was developed to allow the user to easily select reference points/planes/axes to represent the predicted distortion in the selected frame of reference. This feature enables the display of the distortion solution in any frame of reference and enables easy comparison with measured data. In the free-state distortion simulations, six degrees of freedom are removed by assigning boundary condition constrains to the model. Depending on the locations where the boundary condition constraints are applied, the distortion results may appear to be different. For the 2-D example shown in Fig. 11, the distortion results appear to be different with respect to where the constraints are applied. However, if the distorted models are rotated and translated appropriately, the distortion results would be the same. This means that results using different boundary condition constraints can be converted to the same results using a suitable reference frame definition. Various other improvements were made to facilitate the display of distortions in an easily usable format, for example, axial runout display, and so on.

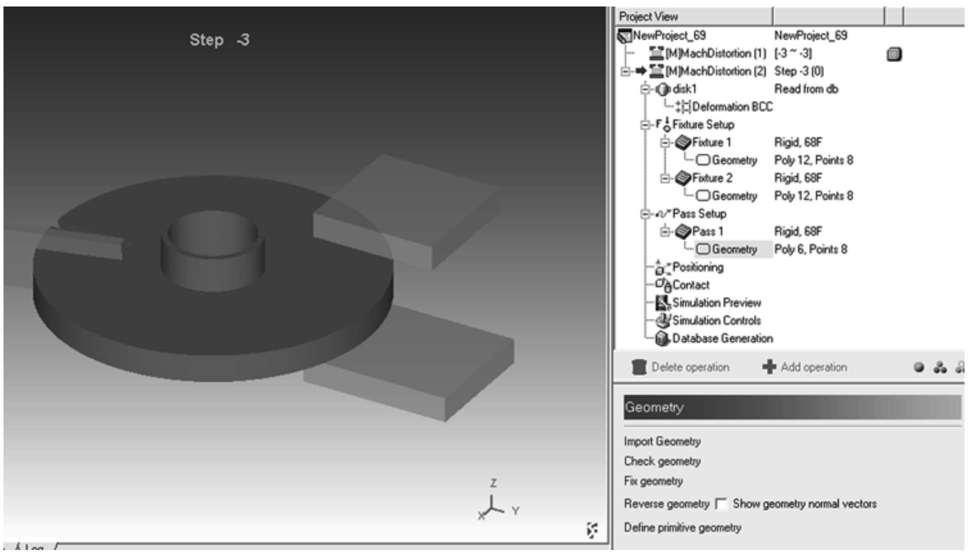

Fig. 8 Machining distortion template

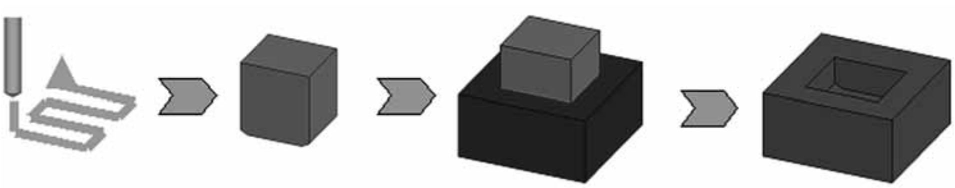

Fig. 9 Boolean geometry creation from machining G-code, material removal, and machined component

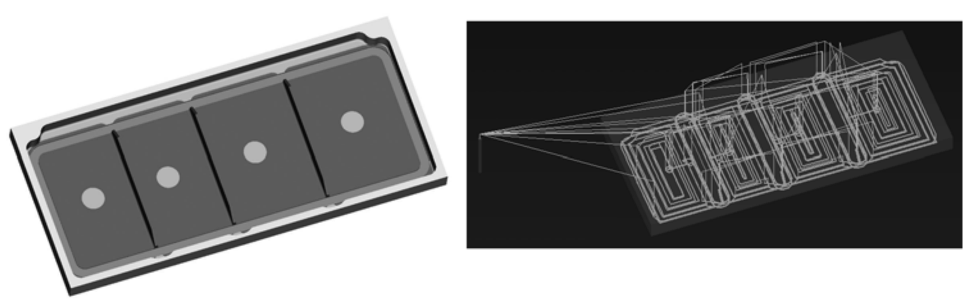

Fig. 10 G-code converter: machining path (G-code) converted to material-removal geometry

Modeling Data Requirements

Material Characterization

The MAI programs have focused on three materials: Ti-64, U720, and alloy 718. However, the model/method is pervasive and can be applied to other materials. The data needed to do this are listed as follows. All data should cover the range from room temperature up to the heat treat temperature:

- Constitutive behavior (stress-strain in plastic region)
- Young's modulus
- Creep and stress-relaxation data
- Poisson's ratio
- Thermal expansion coefficient
- Heat capacity
- Thermal conductivity
- Heat-transfer coefficients during the entire quench process

On-Cooling Tensile Tests

On-cooling tests are used to generate data describing the constitutive behavior of the material: stress as a function of strain, strain rate, and temperature. Data should be generated at a minimum of two different strain rates. Details of the testing procedure are as follows:

- Heat the tensile specimen to the heat treatment solution temperature and hold at this temperature for 20 min.
- Cool the tensile specimen at a specified cooling rate (representative of the cooling rate during the actual quenching process) from the solution temperature to the test temperature, then hold at the test temperature for approximately 10 min for temperature stabilization.

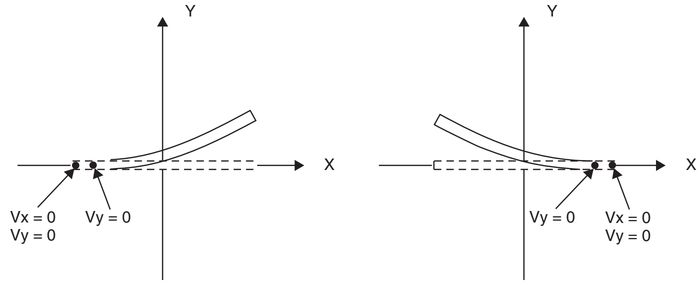

Fig. 11 Two-dimensional illustration showing different distortion results using different constraints

Fig. 12 Heat-transfer coefficient measurement using a disk outfitted with thermocouples

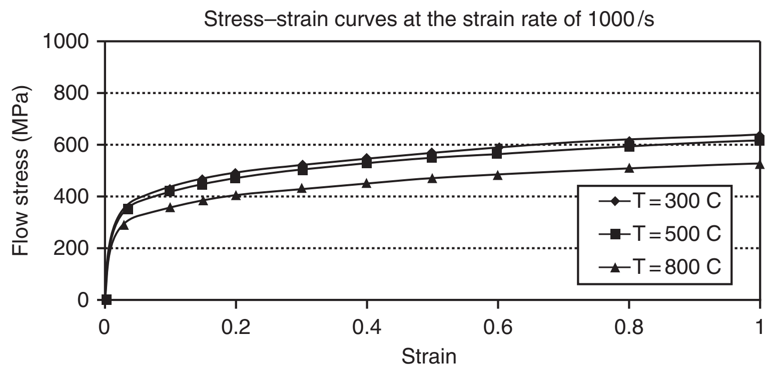

Fig. 13 Typical high-strain-rate flow-stress data

- Conduct tensile testing at this test temperature at a strain rate of 0.005 in./in./min to yield, then at a strain rate of 0.05 in./in./min to fracture.
- This thermal cycling procedure follows the thermal history of the forging during heat treatment, and so, the data generated are representative of the heat treated material.
- Conduct the tests over the temperature range from room temperature to the heat treat temperature.
- These tests give both the Young's modulus and the plastic behavior of the material.

Stress-Relaxation/Creep Tests

There are two methods for generating the data needed for modeling the stress-relaxation behavior during aging. One is to use stress-relaxation curves for the appropriate temperatures and heat treatment condition of the aging cycle. The second is to use data from creep tests. The stress-relaxation test consists of prestraining a tensile specimen to a high elastic strain or just over the yield limit. The displacement is then fixed, and the stress-relaxation curve is recorded for the entire aging time, if possible. Typically for superalloys, stress decreases linearly with log(time). In a creep test, the strain is measured under a given applied stress that is held fixed over time. The stress-relaxation technique requires fewer tests than the traditional creep technique to cover the entire stress/temperature/time behavior of the material. Stress-relaxation curves can be converted to creep strain rate versus stress for use in finite-element models to analyze stress relaxation. It is critical to generate these data with the appropriate microstructure material.

Thermophysical Property Tests

There are ASTM International standard tests for measuring the various thermophysical properties—thermal expansion coefficient, thermal conductivity, and heat capacity—so these tests are not described here (see the Section "Input Data for Simulations" in this Handbook for several articles on thermophysical properties).

Heat Treat Thermocouple Tests

Heat-transfer coefficient data should include transfer from the furnace to the cooling station in addition to the main quench itself (fan, water, polymer, salt, or oil). Typically, the HTCs are a function of temperature and the position on the workpiece. These data are specific to the quench facility used. Accurate HTC data are critical for correctly predicting residual stresses and subsequent machining distortions. The prevalent method of determining HTCs for furnace heatup, transfer, and quench (various media) uses thermal data from a quenching experiment (Fig. 12). This method involves a number of subjective decisions that can significantly impact the accuracy of the results. Inverse methods (2-D or 3-D) for obtaining HTCs are prone to instability and nonunique solutions. Problems exist on the validity of transferring a set of HTCs obtained on one shape to a different shape and in capturing localized distributions at critical geometrical features. An alternative method is to use computational fluid dynamics to predict coolant flow and obtain HTCs using well-established correlations to fluid flow. Computational fluid dynamics has only been used occasionally for this purpose, due to its complexity and lack of accuracy for boiling heat transfer in oil or water quench.

High-Strain-Rate Flow Stress for Machining

For realistic modeling of the machining process, accurate material property data are needed. Flow-stress data are needed over the range of strain, strain rate, and temperature that exist in machining operations. Obtaining the flow stress for use in metal-cutting simulation is difficult because of the high values of strain and strain rate that are involved. Conventional tests (e.g., compression and tensile tests) cannot be used to obtain reliable flow-stress data under cutting conditions. Flow-stress data were measured for mill-annealed Ti-6Al-4V and for alloy 718 by the Engineering Research Center for Net Shape Manufacturing at The Ohio State University. Cutting forces were measured for slot milling tests on plate samples. Flow stress was calculated from the experimental forces and plastic zone thicknesses. The flow-stress data were then validated through finite-element method simulations of orthogonal turning. The advantages of this approach are reduced experimental effort and cost compared to conventional material testing (e.g., compression and tensile tests). Typical high-strain-rate flow-stress data are shown in Fig. 13.

This method is limited by Oxley's assumptions (Ref 1):

- Tool edge is assumed to be sharp.
- Chip formation is of the continuous type (no serrations).
- The width of the cut must be more than 10 times the feed rate to satisfy the plane-strain assumption.

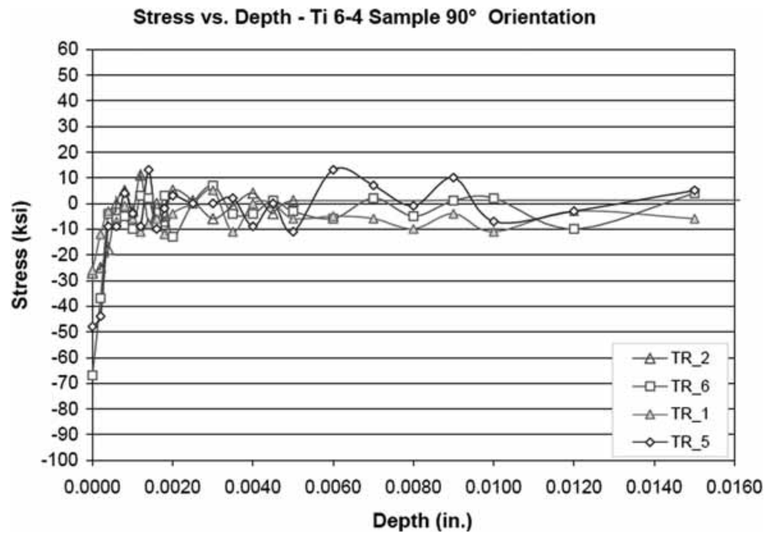

Fig. 14 Residual stresses in the tool axis direction. X-ray diffraction measurements

- Stress and temperature on the shear plane and the tool-chip interface are averaged.
- No built-up edge appears on the tool.

A methodology to obtain flow-stress data suitable for machining simulation using inverse numerical analysis was developed. In the inverse calculation, the error between the measured cutting forces and the forces predicted by DEFORM are minimized using an optimization approach. DEFORM is capable of modeling the machining process in either a transient or a steady-state mode. The steady-state approach is significantly faster (~15 min) than the transient approach (~20 h), with year 2010 state-of-the-art personal computers. The inverse analysis requires multiple simulations to reach the minimum of the objective function (least error between the measured and predicted cutting forces). To shorten the simulation time, the steady-state approach was used to perform the inverse analysis. The 2-D steady-state method was validated by comparing it with the transient approach.

The Johnson-Cook flow-stress equation was used:

$$\sigma_{eq} = (A + B\varepsilon^n) \left(1 + C \ln\left(\frac{\dot{\varepsilon}}{\dot{\varepsilon}_0}\right)\right)\left(1 - \left(\frac{T - T_{room}}{T_m - T_{room}}\right)^m\right) \quad \text{(Eq 1)}$$

where σ_{eq} is the material flow stress; A, B, n, C, and m are five material constants; T is the absolute temperature; T_{room} is the room temperature; and T_m is the melting temperature. (See the article "Evaluation of Workability for Bulk Forming Processes" in *Metalworking: Bulk Forming,* Volume 14A of *ASM Handbook*.)

The procedure was validated using experimental cutting force data from the Aerospace Manufacturing Technology Center. The process was longitudinal turning of a tube made of alloy 718. The inverse analysis was carried out on an Itanium machine, and it took approximately 31 h and 70 iterations to find the minimum of the objective function.

Residual-Stress and Distortion Measurement Techniques

Residual-Stress Measurement

All residual-stress measurement methods are indirect and rely on converting a measured strain (e.g., slotting, hole-drilling, ring-core) to a stress. The inverse procedure leads to high measurement scatter (>100% between different sources and methods) for complicated 3-D stress states. In addition, some destructive measurement techniques can change the residual-stress state as part of the measurement itself. There is an ASTM International standard that outlines the limitations of various measurement methods. Measurement techniques differ in respect of the stress components measured, depth (near surface versus through thickness), mapping dimensionality (1-D, 2-D, 3-D), spatial resolution, sensitivity at low stress levels, destructive versus nondestructive, and near-surface resolution. No single measurement technique is applicable in all cases, and validation requires a combination of measurements depending on component geometry and surface-versus-internal measurements. Validation requirements are dependent on the application requirements (manufacturing distortion, in-service distortion, service-life estimation).

In x-ray diffraction (XRD), the stresses are obtained from the measurement of the crystal lattice strain. The stress obtained is an average over the x-ray beam volume. The accuracy of XRD depends on grain size and therefore the material type. To measure the stress profiles inside or near the surface, some material must be removed to expose the target area. This will affect the stress equilibrium in the component. Therefore, correction methods are needed to obtain the original stress before the material removal. In spite of these limitations, the measurement technique that is most robust for determining the machining stress profile is XRD. However, even this method has the difficulty of collecting data at a sufficient number of points due to the small depth of machining-induced stresses. In addition, it is expensive to gather a large amount of x-ray data.

To test the applicability of the XRD method in measuring machining-induced residual stresses, measurements were performed on four specimens. Measurements were made at 0.0002 in. (5 μm) intervals up to 0.002 in. into the workpiece. Afterward, measurements were made at 0.0005 in. (13 μm) intervals until 0.005 in. Beyond 0.005 in., measurements were taken at 0.001 in. intervals. These results were corrected for material removal at various depths. The XRD measurements indicate high surface stresses but with shallow depth. The stresses do not propagate greater than 0.001 in. below the surface (Fig. 14). With measurements taken at 0.0002 in. depth intervals, only three to five meaningful data points were obtained. The repeat measurement at another test laboratory indicated the same magnitude of stresses but twice the depth of penetration. This shows the uncertainties and variability inherent in all stress measurement techniques. All measurement techniques are indirect and convert a measured strain to stress.

Other less-common techniques can also be employed, such as microslitting, synchrotron, contour method, and so on.

Feasibility Demonstration of Microslot Milling and Distortion Measurement

Tests were performed at Microlution, a designer and builder of micromilling machines, to determine the feasibility of using microslot milling to remove very fine layers of material from the machined surface and to measure the resulting distortion to investigate machining-induced stresses present in the sample. Typically, machining-induced stresses are within the first few hundred micrometers from the surface in titanium. Figure 15 shows a schematic of this process. The sample is clamped near one edge, cantilevering the remainder. First, a measurement device (e.g., confocal laser) is used to measure the initial contour along the path shown by the dotted lines. Next, a small strip of material is removed by micromilling in the form of a rectangular slot the full length of the sample with width w and depth d. The measurement along the dotted lines is then repeated to determine any distortion caused by the layer removal. This process is repeated multiple times to measure the change in distortion caused by each layer removal. The measured change in distortion is related to the removal of machining-induced stresses present in the layer that was last removed and the stiffness properties of the sample.

For aluminum samples, the distortions are approximately 0.005 in. in magnitude. The measurement noise using a laser triangulation measurement system is approximately 0.0001 to 0.0002 in. This provides a signal-to-noise ratio of 50 to 1, and the method is effective. However, the method was not feasible for titanium samples, due to low signal-to-noise ratio at the surface where the larger stresses are located. The sample is stiffest during the removal of the first few layers, when nearly all of the material is intact, and most of the stresses are present in the first few layers. Thus, the distortion measurement is least sensitive in the most critical regime.

Distortion Measurement

When validating the modeling predictions of machining distortions with experimental measurements, the data should be gathered on the face opposite to the one machined in the current operation, before and after this operation. The difference between the before/after measurements gives the distortion induced during this machining operation. This quantity should be compared with modeling predictions. Distinction should also be made between distortion when the component is clamped in the machine fixture versus the free state when all external loads are removed.

If an attempt is made to correlate the modeling predictions of machining distortions with experimental measurements on a face just machined, this can potentially involve large errors. After the workpiece is removed from the fixtures, a free-state dimensional inspection is made. The difference between the nominal undistorted shape and the free-state dimension is the machining distortion induced during this operation. However, in practice, the nominal undistorted state may be slightly offset. Such offsets can occur because the workpiece is not perfectly flat or axisymmetric and cannot be exactly positioned in the fixture on the cutting machine. So, machining distortions induced during the current operation on the cut face are confounded with positioning errors. Axial drops on the just-machined face measured relative to the reference point will be sensitive to the exact amount of material removed and the distortion that occurs as the material is being removed. Therefore, a realistic comparison of the predicted and measured distortions on the just-machined face is difficult.

Dial indicators are the most commonly used for in-process measurement. When the component is still clamped in the fixture, one can use the machine turret to carry a dial indicator to scan the prismatic surfaces and note the distortion contour.

Coordinate measurement machines (CMMs) are also very common for measuring multiple features on more complex parts (Fig. 16). When compared with the modeling results, the model must be in a free-standing state unless the part stays in the same fixture during machining when presented to the CMM.

Optical scanning techniques (laser or fringe projection) have become more mature and more accurate in recent years (Fig. 16). Optical scanning has a unique advantage because it is capable of providing a large amount of digital data of the component profile in a very short time, which none of the other techniques can offer. Because of the size of the *X*/*Y*/*Z* point cloud data file (can be up to millions of data points), special software such as Geomagic, Polyworks, RapidForm, or Surfacers is needed to interrogate the data and compare with CAD models.

Model Validation on Engine-Disk-Type Components

2-D Residual-Stress Validation on Engine-Disk-Type Components

Model validation was conducted first on simple pancake shapes and then on complex production shapes. The experimental heat treat conditions were selected to maximize residual stresses and subsequent machining distortions. The intent was to intentionally generate large residual stresses and machining distortions in order to measure them accurately and to avoid large errors in experimental measurements, which can prevent meaningful model validation. The heat treat cycle consisted of heating the U720 forgings from room temperature to the solution temperature of ~1100 °C (2000 °F), holding at temperature for 2 h, followed by a 30 s transfer time from the furnace to the fan cooling station, then fan cooling for 10

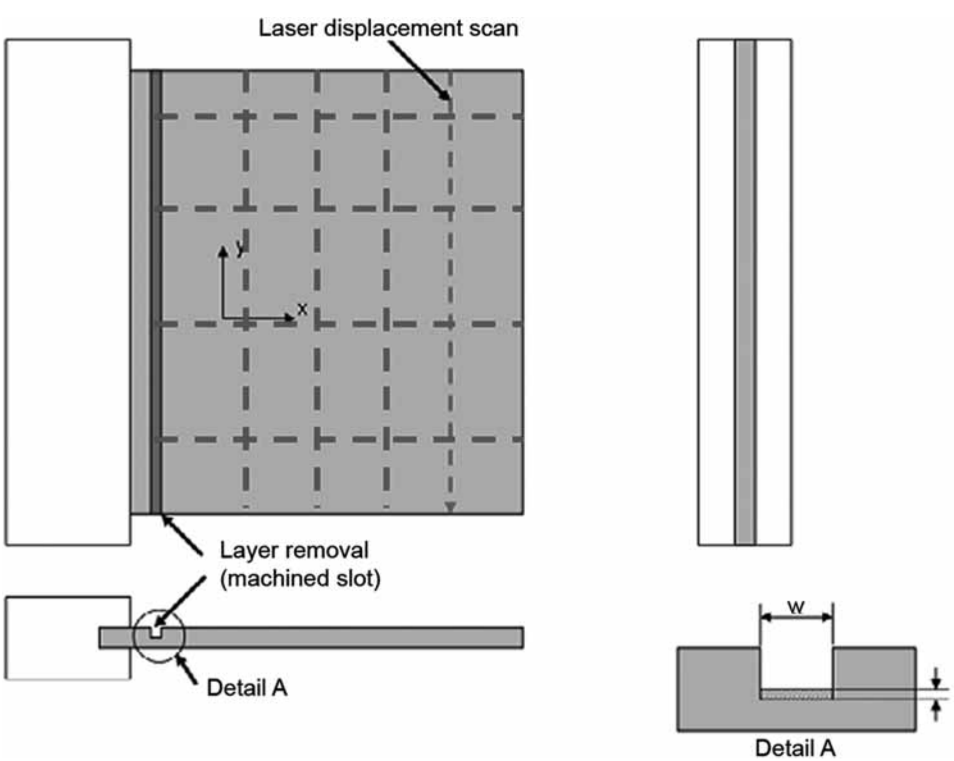

Fig. 15 Layer removal and distortion measurement schematic

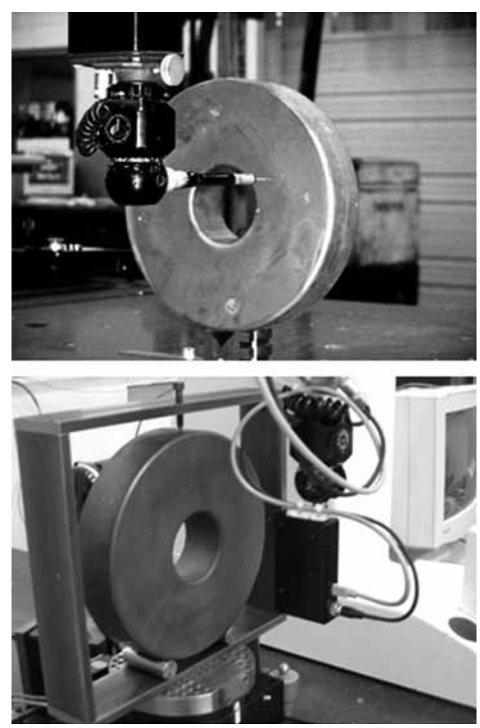

Fig. 16 Coordinate measurement machine inspection and optical scanning setup for measuring distortions

min, after which the forgings were cooled to room temperature in still air.

The heat treatment of a Rolls-Royce production disk (Fig. 17) was performed for two cases: the current oil quench process and a proposed fan quench process as an improvement of the current process. The current production oil quench process has high cooling rates. The proposed fan cooling process results in a close-to-uniform cooling rate in a large volume of the forging of a magnitude that would meet the mechanical property requirements for the disk. This uniformity in cooling rate reduces residual stresses, heat treat distortions, and subsequent machining distortions as compared to the nonuniform cooling rates achieved by the oil quench process. The tensile residual stresses in the middle of the disk are reduced by more than 50% in the fan cooling process as compared to the oil quench process. The heat treat distortion is reduced by approximately 70% in the fan cooling process as compared to the oil quench process.

Residual stresses at the end of heat treatment were predicted. For simplicity, it was assumed that any residual stresses from prior forging operations were not significant and were relieved during the heatup-and-hold stage of solution heat treatment. This assumption is reasonable because the yield stress and creep strength of the material are small at the solution temperature, and therefore, any prior manufacturing residual stresses would be relaxed. The residual stresses in the forgings were primarily induced during quenching. Sensitivity studies were performed to establish that the results were only slightly affected ($\sim$5%) with respect to finite-element mesh size and variations in the HTCs. An uncertainty of $\pm$10% in the HTCs is typical of production conditions.

Given an accurate residual-stress profile, well-defined constraints imposed during machining, accurate material properties, and a well-characterized metal-removal plan, prediction of component distortion should agree reasonably well with measured dimensional changes. However, prior attempts to match measured distortion values against prediction have shown only qualitative agreement. The validation of complex models can easily be frustrated by experimental and analysis inaccuracies as well as by confounding of multiple effects. Therefore, a three-step statistically designed procedure was conducted to validate all the submodules and the overall model:

- Validate the thermal models by conducting thermocouple tests.
- Validate residual stresses and distortions by conducting stress and CMM measurements.
- Validate machining distortions by conducting CMM measurements.

For each step, validation was done in a systematic step-wise manner by testing each feature in the model one at a time and then all together. This helped isolate the shortcomings of the model and remove them before proceeding to an overall validation. Validation was performed on both simple and complex 2-D and later 3-D shapes and on both airframe and engine materials.

First, the thermal model was validated by conducting experiments using a pancake instrumented with thermocouples to measure the thermal response during quench. Heat-transfer coefficients were calculated from the measured temperature-time data. Good correlation was established between simulation and experiment, thus validating the thermal model. The same procedure was repeated on a production shape for both oil and fan quench. The accurate prediction of thermal response is a prerequisite for the accurate prediction of residual stresses and subsequent machining distortions.

Radial and hoop residual stresses were measured along three sections and two clock positions (2 and 10 o'clock) in one pancake forging using XRD.The measurements were conducted up to half the forging thickness. Selected stress measurements were repeated at another test laboratory to evaluate the reproducibility of the measurements and assess the accuracy of the data. The two sets of results differ by approximately 30 to 150%. The accurate measurement of stresses is difficult. Any stress measurement technique is indirect and relies on the measurement of a strain (either by strain gages, hole drilling, chemical milling, x-ray, or neutron diffraction) and converting the strain to a stress measurement. This can lead to large errors in the measured stresses when the state of stress is triaxial with a complicated distribution, as in these forgings. The large differences between the measurements from the two testing sources confirm the inaccuracies involved in the measurement of residual stresses. The validation of the model itself was based on measured distortion data.

A significant amount of material is machined out as the residual-stress measurements are made at increasing depth, as shown in Fig. 18. This material removal will influence the state of stress in the forging. The predicted residual stresses were corrected to account for the material removal. A 3-D 90° model of the forging was created, and the 2-D residual stresses were

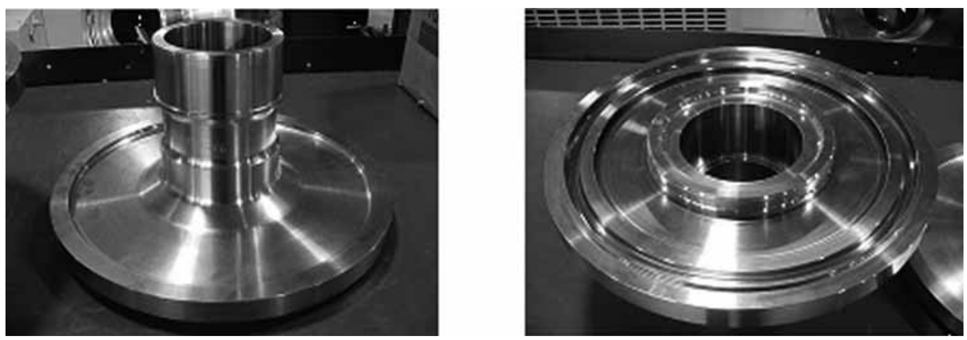

Fig. 17 Machined production disks

Fig. 18 Machining of slots during measurement of residual stresses

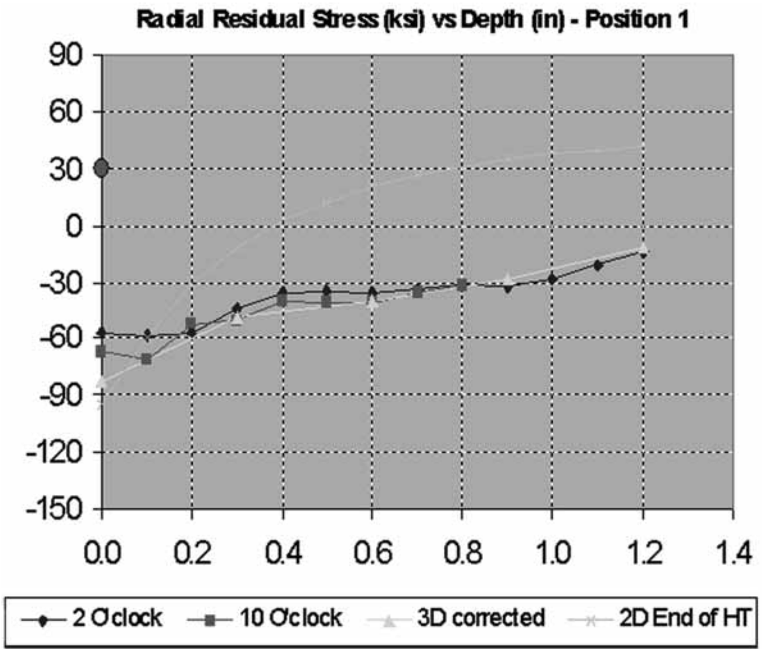

Fig. 19 Comparison of predicted and measured residual radial stress

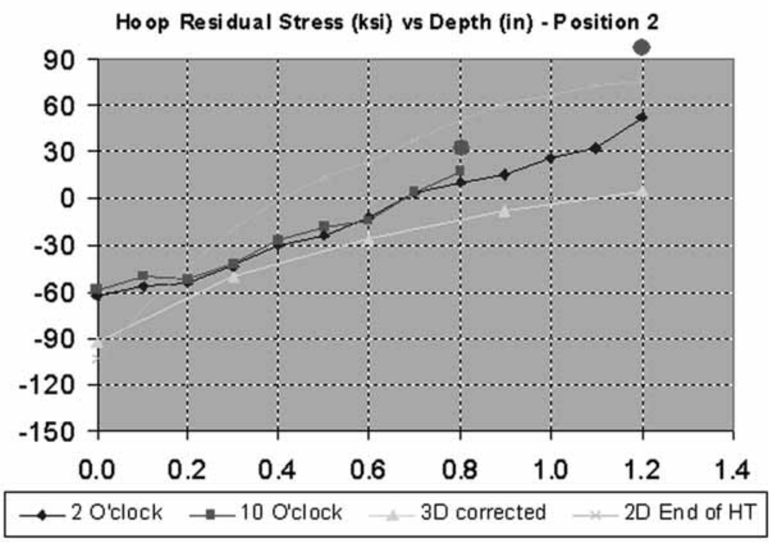

Fig. 20 Comparison of predicted and measured residual hoop stress

mapped onto the 3-D model. In the 3-D model, the machining of the slots was carried out in depths of 7.5 mm (0.3 in.). At each depth, after the material was removed, the stresses and strains were allowed to re-equilibrate. This corrects for the state of stress due to material removal. The predicted stress after successive material-removal passes was compared with measured values to provide a better assessment of the modeling predictions.

Figures 19 and 20 show a comparison of the predicted and measured residual radial and hoop stresses at the three measurement positions. The measurements at the two o'clock and ten o'clock positions are compared with the 2-D predictions at the end of heat treatment and the 3-D predictions corrected for material removal. The 2-D predictions not corrected for material removal do not agree well with the measurements, especially at increasing depth as more and more material is removed. On the other hand, there is good agreement between the measurements and the 3-D corrected predictions. The discrepancy between measurements and predictions is largest at the surface. Possible causes of this discrepancy are residual surface hardening from machining not removed by etching, extrapolation of stresses from the finite-element centroids to the surface, and larger experimental errors near the surface

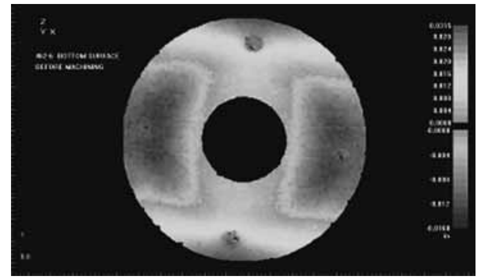

Fig. 21 Optical scan data showing distortions after heat treatment

where the stress gradients are steep. Repeat measurement(s) are shown by closed circles and show the variability between two different measurement laboratories.

2-D Machining Distortion Validation on Engine-Disk-Type Components

Pre- and post-heat treat CMM inspection of the forgings consisted of taking measurements at various radial locations at 45° intervals to obtain the distortion induced during heat treatment (Fig. 21). Forgings that were heat treated identically and also had the same support during heat treat show similar distortions. This demonstrates that the measured heat treat distortions are reproducible. All the forgings had a 3-D warpage as a result of the heat treat process. The measurements for the fan-cooled forgings were more tightly bunched together, showing less 3-D warpage with fan quench as compared with oil quench. The 3-D effect was averaged to allow a comparison with the 2-D cross section results, which are based on the assumption that the component is perfectly axisymmetric (i.e., no warpage). The amount of nonaxisymmetry decreases as the machining progresses. Note that the distortions are almost axisymmetric after machining. The nonaxisymmetry introduced during heat treatment has been removed during machining.

The measured distortions are the result of deformations occurring during heatup from room temperature to the solution temperature, holding at solution temperature, and subsequent quenching back to room temperature. The meaningful validation of predicted heat treat distortions is confounded by the interplay between several factors and by the fact that the distortions are small (~0.25 mm, or 10 mils, generally). The modeling predictions show the distortions induced only during the quenching part of the process. The measured and predicted heat treat distortions do not show good agreement, because the distortions occurring due to creep and sagging during heatup and holding have been ignored in the model. The modeling of these distortions requires creep material property data at high temperatures and the inclusion of gravity-induced sagging. This influences the distortions strongly. However, because the internal residual stresses are relieved during holding at solution temperature and regenerated during the cooling process, this assumption has a negligible effect on the prediction of residual stresses and subsequent machining distortions.

For the pancake forgings, the finished shape shown in Fig. 22 was chosen for the purpose of achieving large distortion (for easy measurement). The material was removed in the four quadrants (top/bottom, inside diameter/outside diameter). Several alternate machining shapes were investigated, and this one was chosen to obtain distortions in the 10 to 20 mils range.

Fig. 22 Forging of U720 after all four quadrants have been machined

Distortions in this range are required in order to measure them accurately and to avoid large errors in experimental measurements, which can prevent meaningful model validation.

Initial predictions of machining distortions showed poor agreement with the measured data. For some cases, the predicted distortion was in a direction opposite to that measured. Measurements showed that the distortions caused by clamping forces while the forging was machined were negligible. All modeling inputs and procedures were examined carefully, and five improvements were made to obtain better agreement between the measured and predicted residual stresses and machining distortions:

- Exact stress-strain behavior instead of a simplified bilinear representation
- Strain-rate dependency of stress-strain data
- Material removal in layers versus single pass to predict the correct distortion direction
- Kinematic versus isotropic hardening
- Temperature-dependent Poisson's ratio

Of these five changes, the first three had the most significant effect on modeling predictions. The last two had a smaller effect. The plots shown in Fig. 23 to 25 are a small sample of all the results and show the general behavior. These figures show, in general, a good agreement between the predicted and measured machining distortions, considering the extent of nonaxisymmetric deformation at some operations. In most of the cases, the agreement is within $\pm 20\%$. When the distortions are very small (<5 mils), the noise in the measurements is large relative to the measurement. This can show up as a large percentage error but small absolute error. Process improvements by changing the machining sequence have been demonstrated using the model and were implemented successfully, resulting in cost-savings.

The conclusions of the distortion validation study are:

- Distortion measurements are more reliable and were used for model validation.
- Measurements and predictions show the same trend for all cases.
- Predictions agree better with measurements for smaller depths of cut.
- Predictions agree better with measurements for oil quench than for fan quench.
- Moving the finished shape axially changes the distortion approximately the same as the 3-D variation.
- The machining distortions are ~50% less with fan quench than with oil quench due to reduced residual stresses. This is a potential process improvement.
- Possible reasons for the discrepancy include:
  a. 3-D heat-transfer coefficient variation not exactly captured in the 2-D axisymmetric model
  b. Inaccuracy in extrapolated low-strain-rate stress-strain data
  c. Sag in the furnace: effect of heat treat fixtures

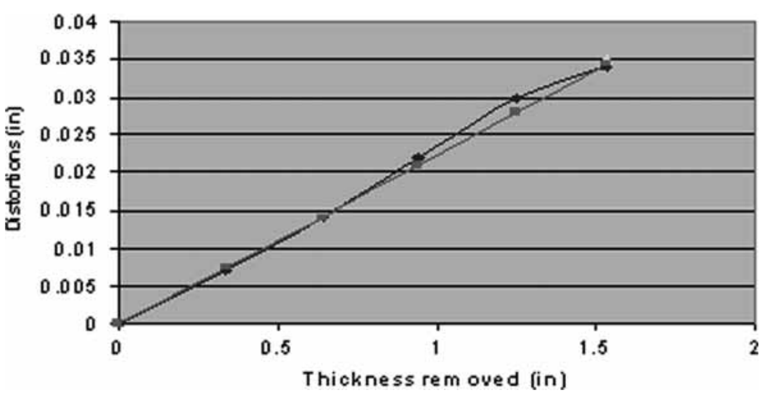

Fig. 23 Comparison of measured and predicted distortions for pancake forgings

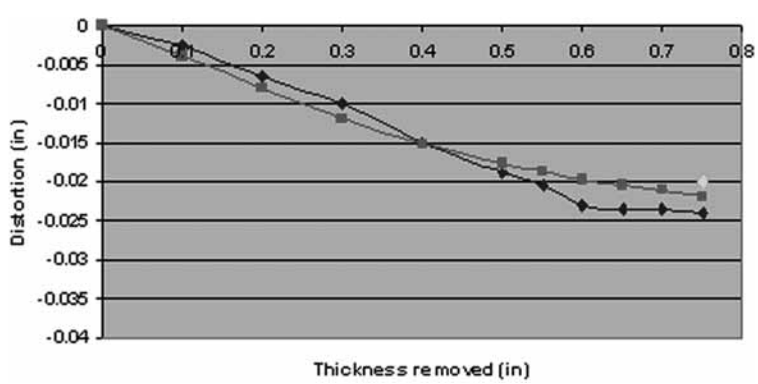

Fig. 24 Comparison of measured and predicted distortions for pancake forgings

In practice, material is removed on one side of the component, the component is flipped over, and material is then removed on the other side. This process is repeated until one gradually approaches the finished component shape by successively removing smaller amounts of material on each side. This requires a number of machining operations, especially for distortion-prone geometries and/or materials. A possible machining strategy is to model the material removal to increasing depths on one side, up to the point where there is positive material left over the finished component shape. At this point, the forging would need to be flipped over and the process repeated on the other side.

2-D Machining Distortion Validation using National Aeronautics and Space Administration Data

The National Aeronautics and Space Administration's (NASA) Integrated Design and Processing Analysis Technology and Advanced Subsonics Technologies programs studied residual stress and machining distortions in advanced disk alloys. This work was extended to predict the effect of heat treatment on residual stress and

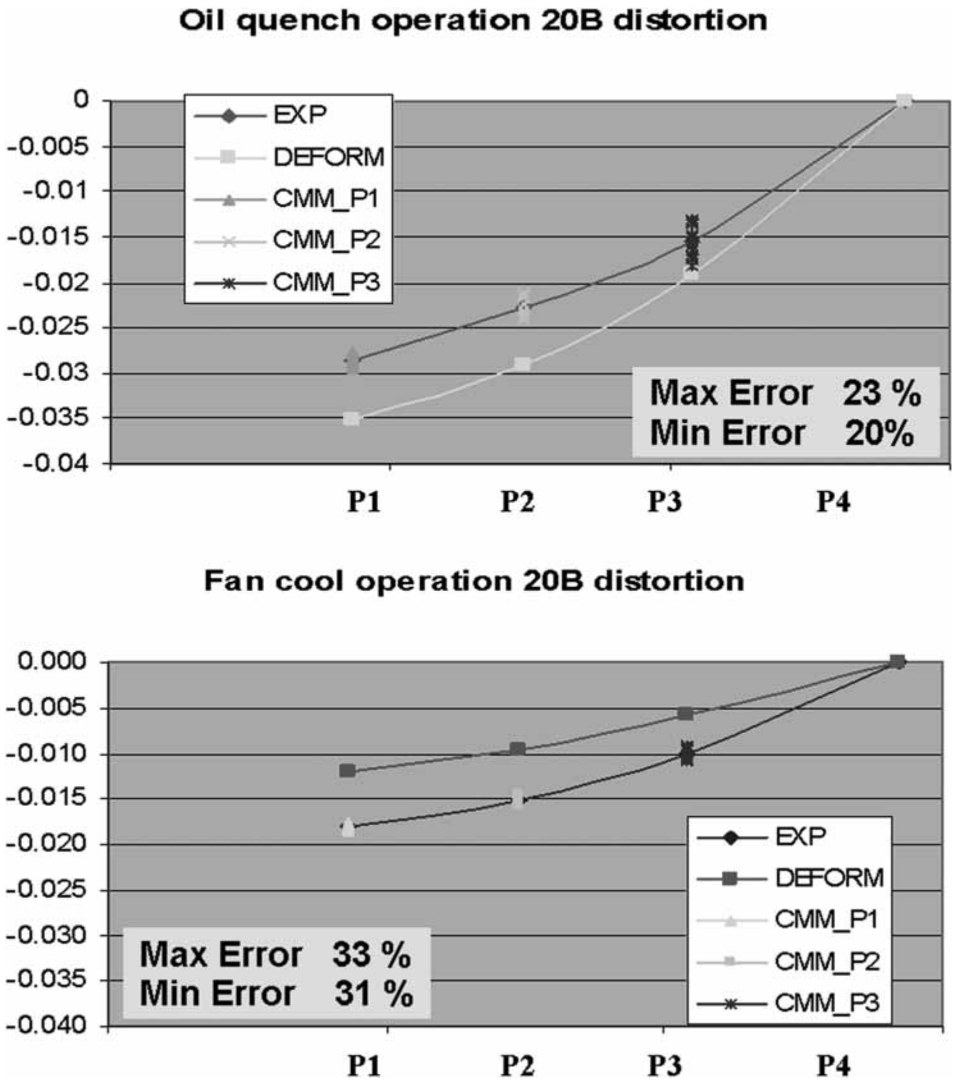

Fig. 25 Machining distortions: fan vs. oil quench. Distortion data represent the average of the eight experimental measurements at 45° intervals. The data points (coordinate measurement machine, CMM) show all eight measurements and the extent of nonaxisymmetric distortion. DEFORM represents the modeling predictions

subsequent machining distortions of simple forgings made of an advanced disk alloy (Ref 2, 3). Four pancake-shaped disks, weighing approximately 45 kg (100 lb) each, were isothermally forged to a pancake shape 35 cm (14 in.) in diameter by 4.8 cm (1.9 in.) thick. The four forgings were given different heat treatments. Heat treatments 2, 3, and 4 produced a fine-grained microstructure as a result of subsolvus solution temperature (1135 °C, or 2075 °F) and were designed to yield progressively lower residual stress. The first heat treatment produced a coarse-grained microstructure as a result of the supersolvus temperature (1182 °C, or 2160 °F) and was included to provide a direct comparison with the subsolvus, stabilized heat treatment. The dimensions of the four forgings were measured to obtain the initial distortion/warpage resulting from heat treatment.

DEFORM was used to simulate the four heat treatments to predict the initial residual-stress distribution prior to machining. Following this, two machining operations were performed (Fig. 26), which consisted of two face cuts on the top surface of each forging. The first cut went to a depth of 0.24 in. (6 mm), and the second cut went an additional 0.24 in. for a total depth of 0.48 in. After each cut, the disk was unclamped, and warpage and thickness measurements were made. These data were gathered under controlled conditions for multipass machining operations and are therefore very suitable for model validation. Figure 27 shows a comparison of the axial distortion data measured by NASA (dotted lines) and the simulation data from the DEFORM (solid lines) machining distortion model. The measurements show that the disks are not perfectly axisymmetric. The measured distortion is an average of the eight sampling points around the circumference. The agreement between measurements and predictions is very good. Similar good agreement was obtained for the distortion of the other disks, also.

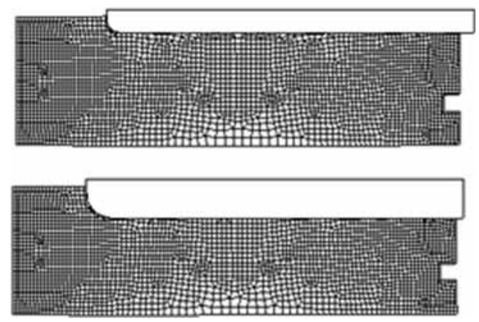

Fig. 26 Two machining operations

3-D Model Validation on Engine-Disk-Type Components

The machined U720 forging shown in Fig. 22 was selected for broaching distortion validation. The heat treatment and prior machining of this forging had been well characterized. Several simulations were carried out to define the machined geometry that would result in measurable distortions. Distortions should be large enough so that they can be measured accurately and used meaningfully for model validation. Small distortions are likely to have noise in the data, making such data unsuitable for model validation.

Two slots, each 5 cm (2 in.) deep, were broached in the U720 disk (Fig. 28). These slots simulate dovetail slots for blades in aircraft engine rotating disks. This was a well-controlled experiment to generate meaningful data for model validation. The finite-element mesh was fine in the vicinity of the slot to accurately capture the stress and distortions in this region. Radial, axial, and hoop distortion measurements were taken in the slot region after the machining of each slot.

Two tapered pockets with a wall thickness of 0.5 cm (0.2 in.) were milled in another U720 forging (Fig. 29). These pockets simulate features in airframe structural components. The pocket wall thickness was large enough to avoid distortions induced by cutting forces and surface residual-stress effects. The finite-element mesh was fine in the vicinity of the pockets to accurately capture the stress and distortions in this region. Radial, axial, and hoop distortion measurements were taken in the slot region after the machining of each pocket.

Model validation was completed on experimental 3-D shaped components similar to production forgings. Alloy 718 pancake forgings were made from 20 cm (8 in.) billet weighing 55 kg (120 lb) and forged to ~35 cm (14 in.) in diameter and 5 to 7.5 cm (2 to 3 in.) thick. One forging was used for gathering temperature data during quench for obtaining HTCs. Figure 30 shows the comparison between measured and predicted temperatures at two thermocouples representing the best and worst matches. This figure also shows the layout of the thermocouples. A total of 13 thermocouples were used to capture the HTC variations around the forging.

Production disklike features were machined in four forgings, modified to accentuate the machining distortions: dovetail slots in the rim, holes in the web, and stem slots (Fig. 31). Prior to machining the forgings, the process was modeled to define the machined geometry and machining sequence. The objective was to define conditions that would result in measurable distortions. Distortions were measured at each machining step. The measured distortions of each disk were compared to the corresponding numerical prediction. Much data were gathered at all steps of machining. Here, only the distortions introduced during the 3-D machining steps are shown for the four disks.

A comparison of the measured and predicted distortions at the stem (disk 1) and at the outside diameter (OD) (disk 2) is shown in Fig. 32. A comparison of the measured and predicted distortions at the OD (disk 3) and at the stem (disk 4) is shown in Fig. 33. In all cases, the measured and predicted machining distortions matched within $\pm 30\%$ on average.

Thermocoupled trials, residual stress, and machining distortion analyses have been completed on various production aircraft engine disks at the various original equipment manufacturers. The modeling results were generally in good agreement with the measurements.

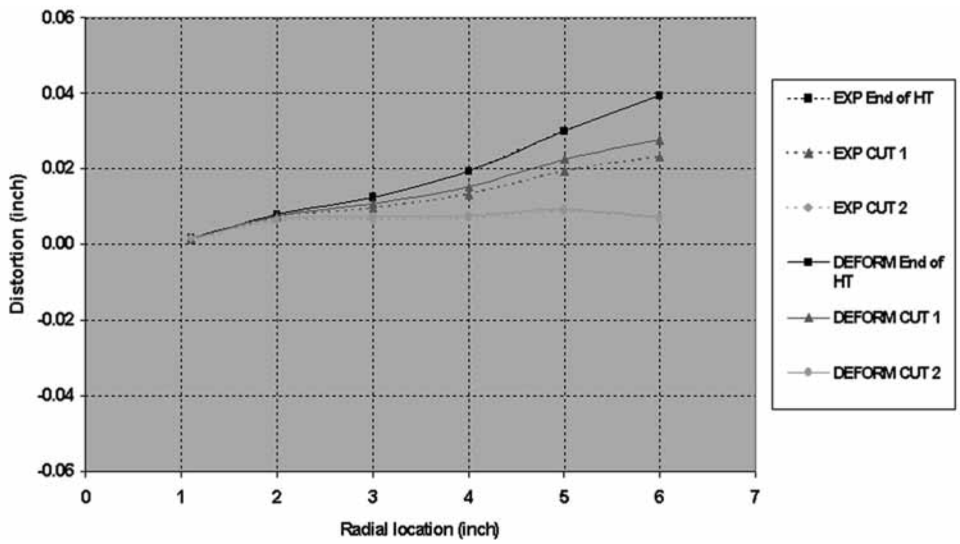

Fig. 27 Good agreement between DEFORM predictions (solid lines) and NASA's measurements (dotted lines) of the axial distortions of disk 1 after heat treatment and after two machining cuts

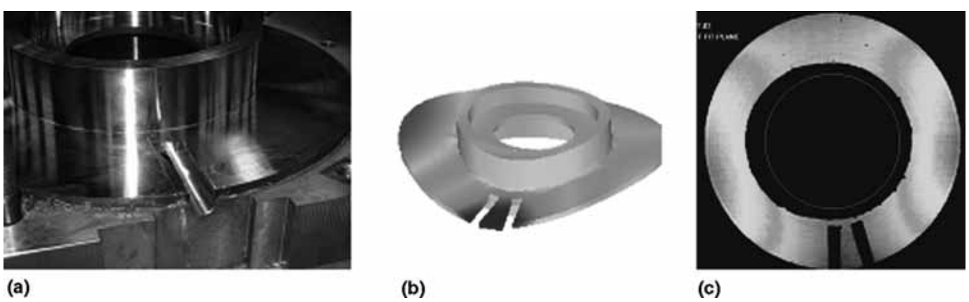

Fig. 28 Good agreement between predicted and measured distortions in U720 after slot broaching. (a) U720 forging being machined. (b) Predicted axial distortion. (c) Measured distortion

Machining-Induced Residual Stresses and Distortions

For airframe-type components, machining-induced surface residual stresses are generally the main cause of distortions. The 3-D process model predicts component dimensional changes as a function of the initial residual-stress state, cutting tool forces, machining-induced surface stresses, machining plan design, and machine fixtures. Measurement and modeling of machining-induced residual stresses and distortions in subscale rib/web geometries were performed. Machining-induced residual stresses were obtained from one of four methods:

- *Detailed finite-element analysis of the cutting process:* Slow, expensive to run, reasonable accuracy
- *Simple fast-acting mechanistic model:* Fast, cheap to run, reasonable accuracy after calibration
- *Semiempirical linear stress model:* Fast, cheap to run, good accuracy after calibration
- *X-ray diffraction measurements:* Empirical, slow, expensive

The first three methods are described in the following sections. X-ray diffraction measurements have already been described in the preceding sections. Stresses from these models

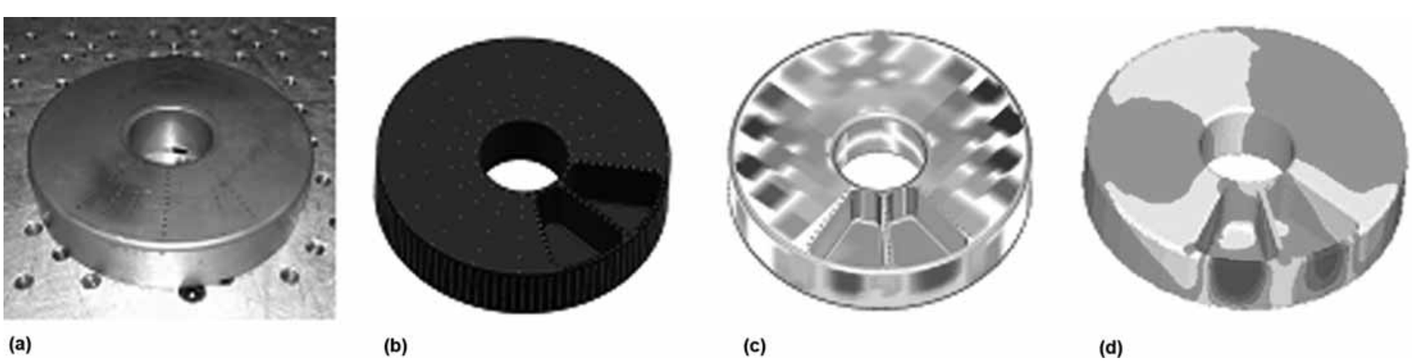

Fig. 29 Good agreement between predicted and measured distortions after pocket milling in U720. (a) U720 disk. (b) Measurement holes. (c) Measured distortion. (d) Predicted distortion

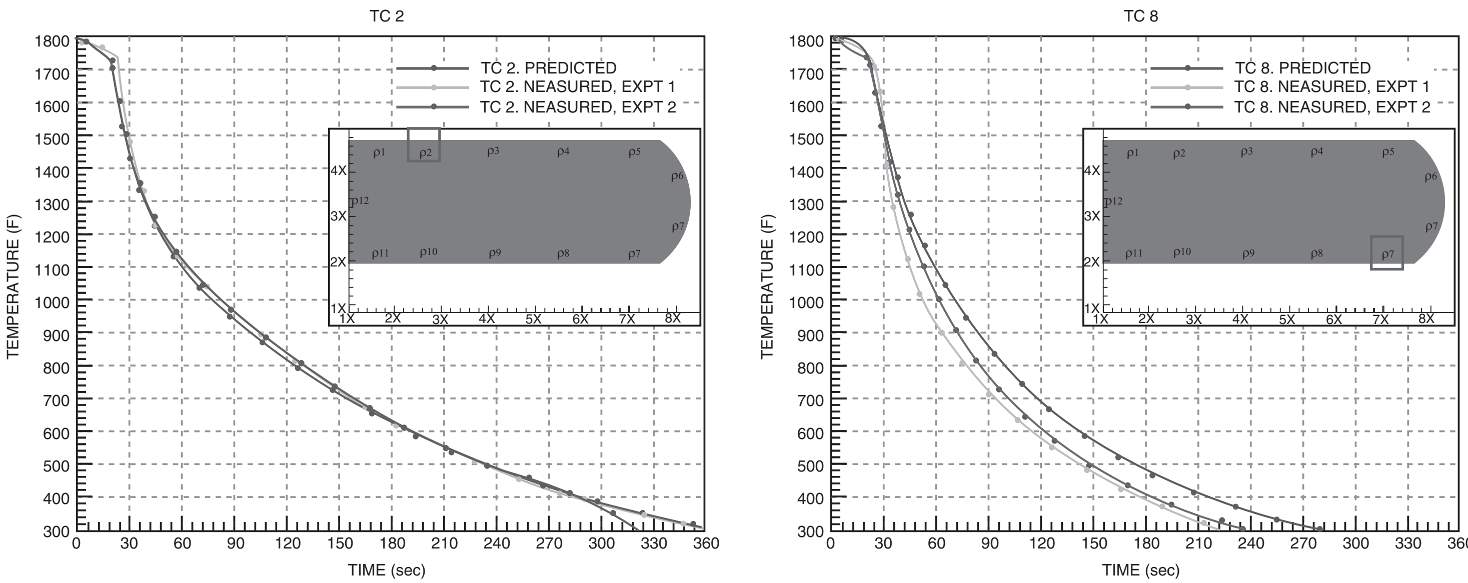

Fig. 30 Comparison between measured and predicted temperature during water quench: thermocouples (TC) 2 and 8

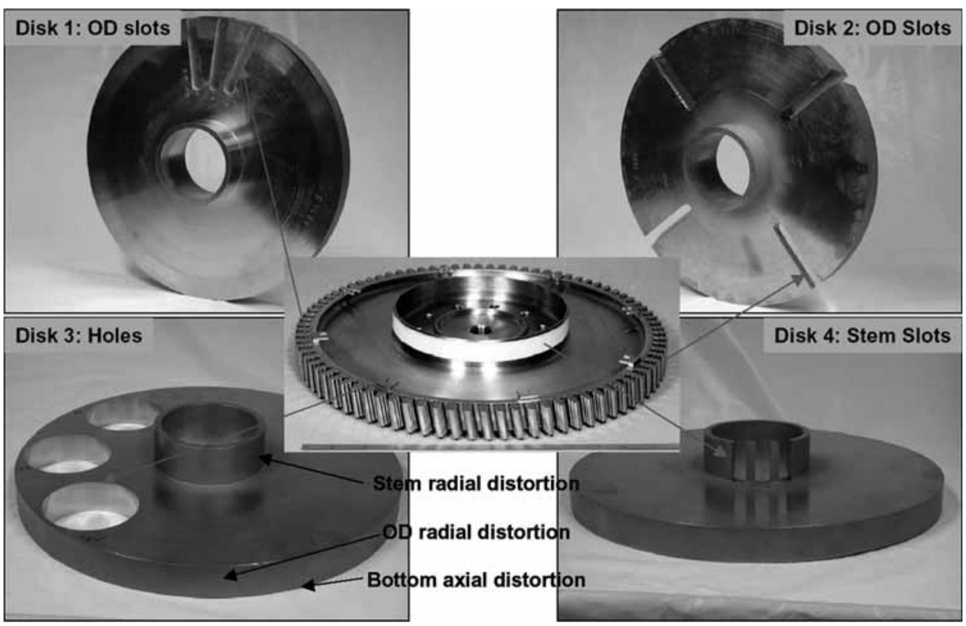

Fig. 31 Machining of production-like features in engine-disk-type forgings. OD, outside diameter

and/or measurements were input into a 3-D distortion finite-element model to predict component distortion. Distortion data were gathered after machining and compared with the modeling predictions.

Finite-Element Prediction of Machining-Induced Stress

Detailed finite-element modeling of the machining process can be performed using commercial software such as DEFORM or AdvantEdge (Third Wave Systems). Here, results from AdvantEdge are reported. Simulations were performed using AdvantEdge for selected conditions of cutting speed, feed, radial and axial depths of cut, cutter geometry (including edge preparation, axial and radial rake angles, number of flutes), and material grade. The simulations predict temperatures, forces, and machining-induced residual stress. The tool used had a 35° helix angle, 8 flutes, a 19.05 mm (750 mils) diameter, with a 3.048 mm (120 mils) corner radius and an edge sharpness of 0.0508 mm (2 mils).

Hole-drilling measurements were conducted at Los Alamos National Laboratory (LANL). The error for each measurement was estimated as 5% by LANL, based on historical evidence, with the exception of the first measurement (0.05 mm, or 2 mil, depth), which was estimated to have a 10% error due to the dish angle of the drill. Due to the nature of the hole-drilling experiments, axial stresses could not be obtained, and the first point measured was at 0.05 mm depth. Figure 34 shows a comparison of the predicted and measured tangential and radial stresses for a cutting speed of 121 surface meters per minute (smm) and a feed of 0.0508 mm/tooth. Both exhibit maximum compressive stress values at approximately 0.05 mm; however, the simulation results underpredict the magnitude compared to the measurements.

AdvantEdge 3-D predictions satisfactorily captured the effects of variations in chip loads and cutting speeds on the workpiece residual stresses. Trends of peak stress as a function of feed and speed were similar between the simulations and hole-drilling measurements. Cutting speeds were observed to have a significant effect on surface stresses in the simulations. With increased cutting speed (and correspondingly higher temperatures on the tool and workpiece), the surface residual stresses were observed to increase and become more tensile. Increased chip loads (feeds) were observed to have a pronounced effect on subsurface stresses. With increased chip loads, subsurface stresses (below peak compressive zone of stresses) were observed to become less compressive in nature. Mesh refinements did not result in a substantial change in the predicted results.

Detailed finite-element models of the chip formation process are time-consuming to run and are not yet fully validated. Meaningful results can be obtained if the cutting process can be approximated as 2-D (e.g., turning), with computational times of 4 to 8 h. For 3-D cutting processes, several days of computational time are required. Therefore, these models are not yet production-ready to be used in the industry on a routine basis.

Mechanistic Machining Model

Mechanistic machining models have been developed for quickly predicting (in seconds as opposed to several hours or days for finite-element methods) cutting forces, temperature, and machining-induced residual stresses for broaching and milling processes. The speed with which these models generate results provides the potential for analyzing a wide range of conditions in a short period of time to establish a set of conditions for use in a production environment. The overall procedure consists of obtaining cutting forces from the mechanics of cutting, computing stresses from the applied cutting loads, and relaxing the stresses to obtain the residual stresses in the workpiece (Ref 4). Mechanistic models must be calibrated with experimental data and are good over a limited range of cutting conditions close to the calibration data set. The models predict the cutting forces reasonably well for both broaching and milling operations. The residual stresses are captured with respect to trends and depth of penetration.

Linear Stress Model

Samples of ribs and webs that are representative of large airframe structural components were used to evaluate machining-induced residual stresses and distortions. The principal stresses for rib coupons are aligned with the helix angle of the cutter. For the web coupons, the principal stresses are aligned tangential and normal to the cutter radius. Process parameters used as control variables included spindle speed, feed rate, cutting tool material, cutting tool geometry, and edge sharpness, which were defined using Taguchi methods. Ribs were made by finishing with the side of a cutter, and webs were made with the bottom of a cutter. The geometry was chosen to allow a 5 by 5 cm (2 by 2 in.) sample for stress and distortion measurement. Industry-standard milling cutters were selected to machine the samples (Fig. 35).

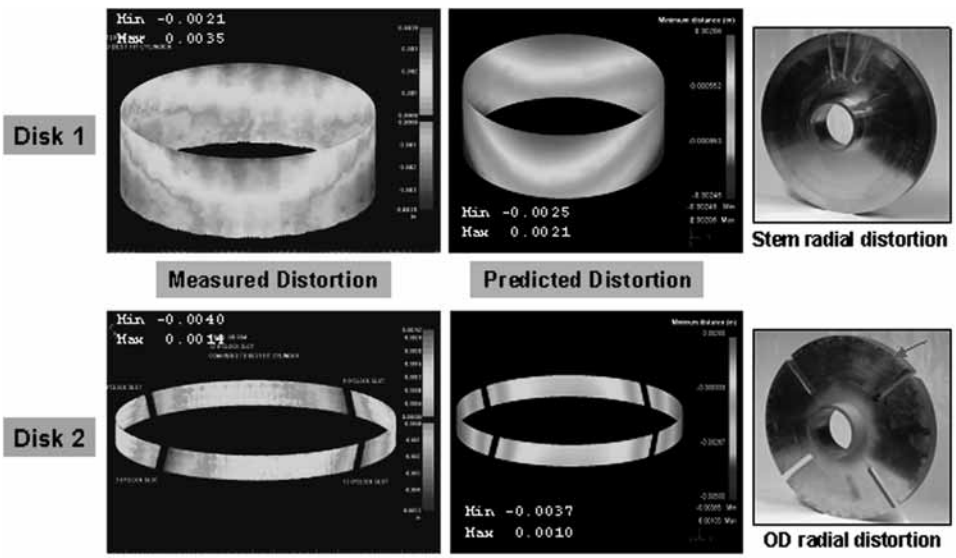

Fig. 32 Comparison of measured and predicted distortions for disks 1 and 2. OD, outside diameter

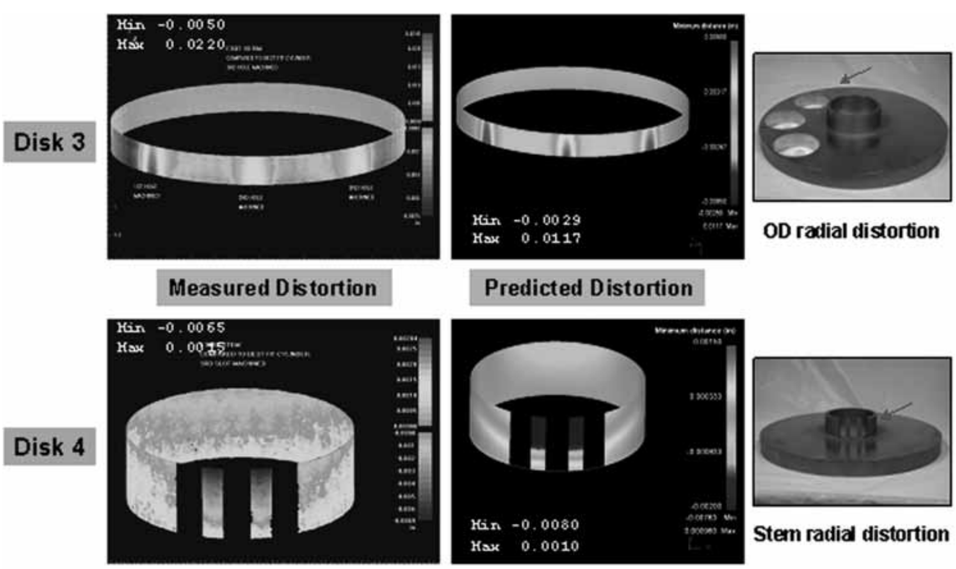

Fig. 33 Comparison of measured and predicted distortions for disks 3 and 4. OD, outside diameter

A thin sample distorts after machining, thus relieving some of the machining-induced stresses. Therefore, the residual stress measured in a thin sample is not the same as the machining stresses. To accurately measure the machining-induced stresses, samples much thicker than typical thicknesses were used. This eliminates the postmachining distortion and partial relief of stresses and accurately captures the stresses induced by machining.

Based on the rib and web distortion experimental data, a linear stress model was developed for the mapping of residual stresses on an airframe-type component and for obtaining its distortion due to machining-induced residual stresses. Based on experimental and numerical observations, the following assumptions were made:

- Machining-induced effects are concentrated in a thin surface layer.
- Machining-induced effects from previous cuts are removed, and a new surface stress layer is created during each pass of the tool. Therefore, only the machining parameters in the last pass are needed to determine the machining-induced effects.
- Machining stresses depend on the thickness direction only and can be averaged over the machined surface.
- Machining-induced plastic strains do not depend on the shape of the component for a given set of tools, material, and machining parameters.
- Machining-induced effects at joints (e.g., filleted regions) are not significant and therefore are ignored for the determination of distortions and residual stresses.

The distortion of the rib and web samples was measured using laser interferometry. The measured distortion was fitted with polynomial functions (linear coefficients for the *x*-, *z*-, and *xz*-directions). The three coefficients represent bending in the two directions and the twist, respectively. Figure 36 shows the contribution to the distortion caused by each one of the linear terms (*x*, *z*, and *xz*). The ability to obtain a good fit of the distortion using linear terms indicates that the linearity assumption is valid.

Coupons with a worse fit had small distortions with a small signal-to-noise ratio.

For a component that is a collection of ribs and webs of relatively uniform thickness joined by fillets, the distortion can be predicted by using as input linear terms determined through the experiments described here. Based on risk, cost, and schedule feasibility, for production use, an empirical combination of XRD with calibration by linear stress modeling was selected.

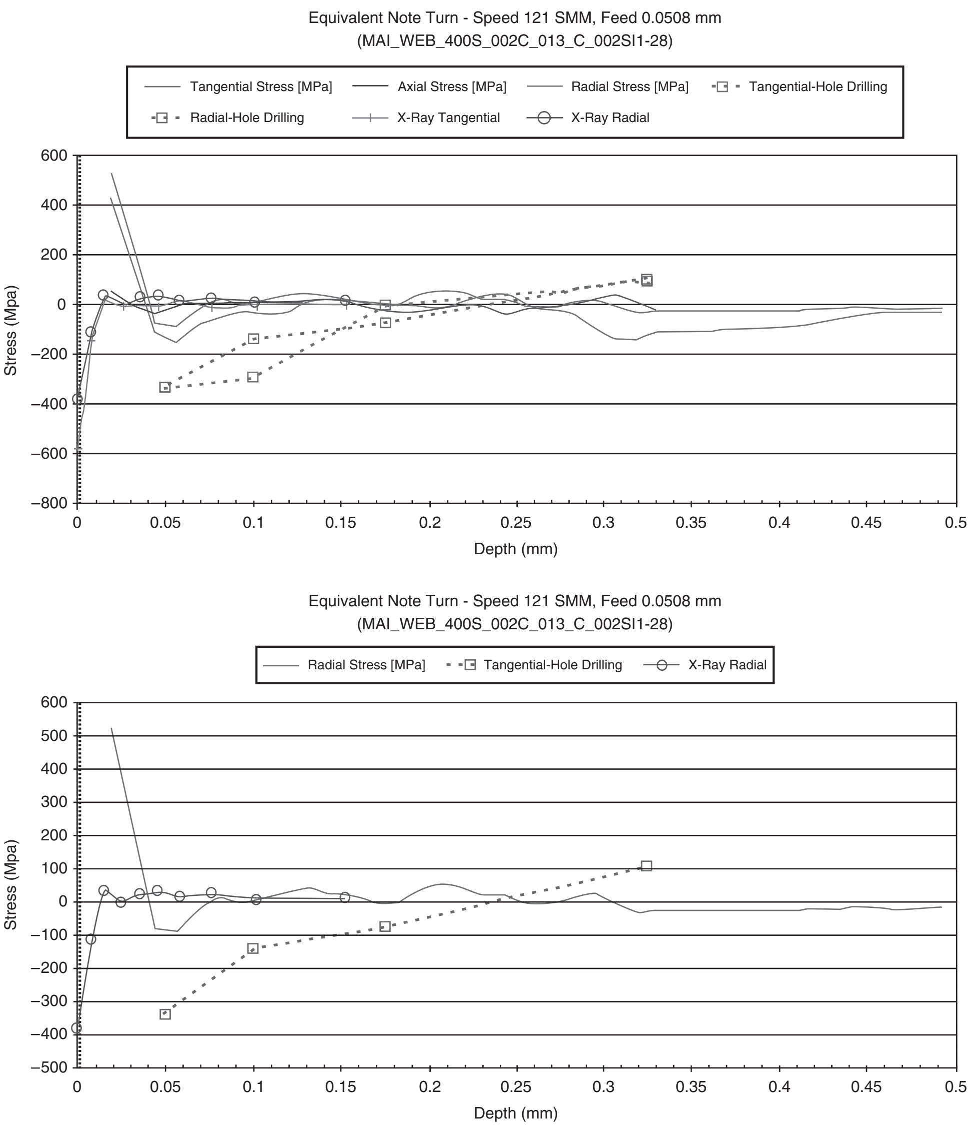

Fig. 34 Turning/hole-drilling comparison for a cutting speed of 121 surface meters per minute (smm) and a feed of 0.0508 mm/tooth

Fig. 35 (a) Tungsten carbide and AISI M-42 cutting tools. (b) Machining of subscale webs. (c) Machining of subscale ribs

This approach combines the best measurement of the shape of the machining stress profile (x-ray) with the best measurement of the magnitude of the machining stress profile (linear stress model). The x-ray data defined the shape of the stress gradient as starting negative (compressive) and quickly decaying to zero. The coefficients in the linear stress model were obtained by matching the area under the stress profile (weighted by the distance normal to the surface). Figure 37 is one example of the stress input.

Four rib and four web coupons were modeled (Fig. 38, 39). The dimension of the rib and web coupons was 5 by 5 cm (2 by 2 in.). The thickness of the coupon was assumed to be uniform. Eight-noded linear brick elements were used. Surface meshes were generated to capture the initial stress variation through the thickness direction. Six nodal points are enough to capture this input curve. The coupon was then allowed to re-equilibrate under the applied stress field. The resulting distortion was compared with the measurements. Numerical tests were conducted to evaluate the effect of mesh size on the distortion results. Increasing the number of thickness layers had minimal impact on the results. However, increasing the number of in-plane elements had a significant impact. A mesh size of 96 by 96 in-plane elements with 12 thickness layers provided a mesh-independent converged solution.

The model was validated on a selected subset of rib/web samples using residual stresses from a mechanistic model and from x-ray measurements. Figure 40 shows a comparison between the measured and prediction distortions for typical rib and web samples. The ribs twist and the webs bow out, which is consistent with prior experience. The error between the predictions and the measurements ranges from 2 to 29%. Similar agreement was obtained on production components that cannot be shown here due to proprietary reasons.

Integration of Machining Stresses into DEFORM

Inclusion of surface stresses and cutting tool forces is important for components with thin section sizes. Figure 41 shows a flow chart of the production distortion model. The machining stresses are imported into DEFORM using a graphical user interface (GUI), taking into account the cutter direction, path, and type. The GUI enables easy, error-free import of data. Bulk residual stresses, if significant, can be superposed on the machining stresses. The overall stress field is then equilibrated to obtain the component distortion. If the distortion is outside prescribed limits, the process is repeated with a different machining process until the distortions fall within the prescribed limits.

The simulation procedure consists of these steps:

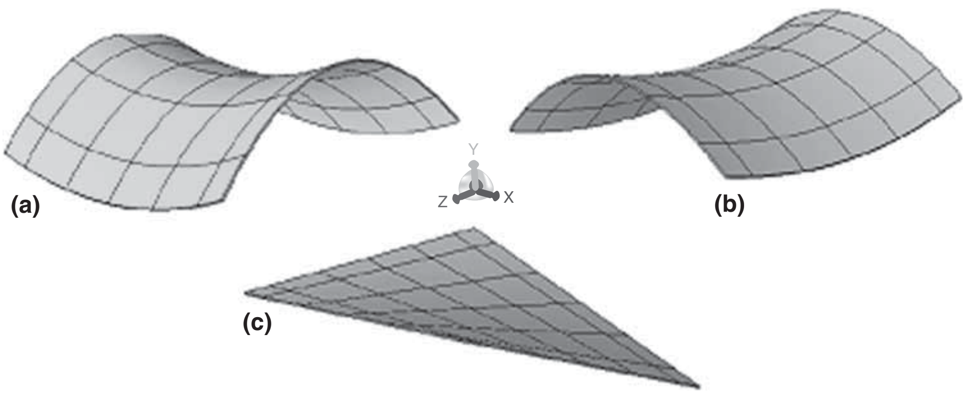

Fig. 36 Displacement computed for linear shape functions. (a) *x*-component. (b) *z*-component. (c) *xz*-component

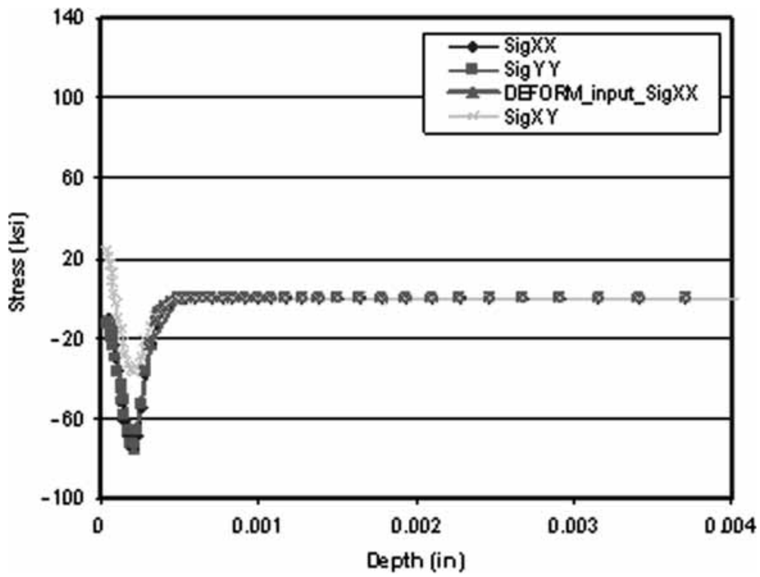

Fig. 37 Example of stress input curve

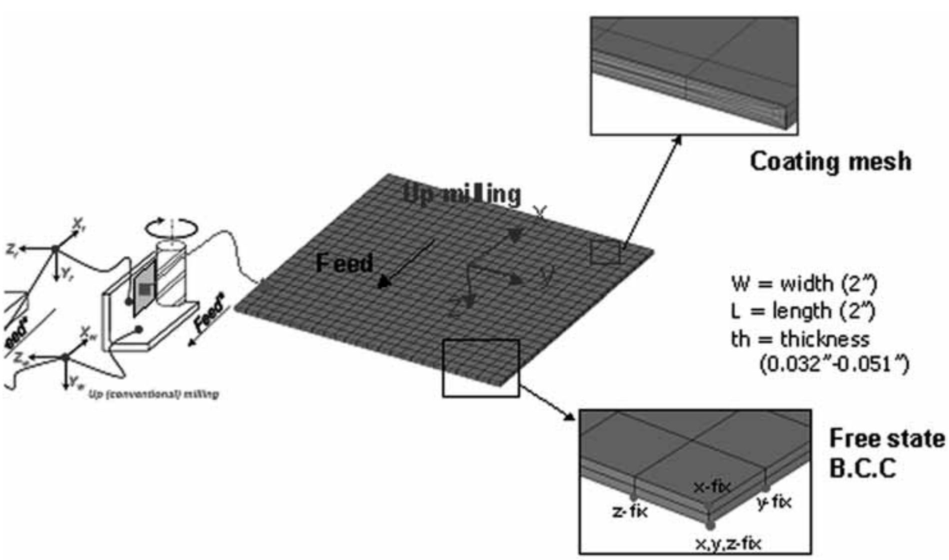

Fig. 38 Finite-element model for rib coupons. bcc, body-centered cubic

1. Generate a brick mesh for the final machined component.
2. Generate multiple layers of near-surface mesh to capture the machining stresses.
3. Interpolate bulk residual stress from heat treatment to this mesh, if needed.
4. Import machining-induced residual stresses to the near-surface mesh (details follow).
5. Carry out a stress equilibrium simulation.
6. Repeat the process for subsequent machining operations, if needed.

The following procedure was developed for importing cutting-induced residual stress:

1. Generate a fine surface mesh.
2. Pick surface nodes in the region where the stresses are to be imported.
3. Input cutting direction for the region.
4. Define machining-induced residual stress as a function of depth or a constant value.
5. Interpolate imported stress components to the mesh nodal locations. Rotate the stress components to the model coordinate system. The rib region is cut by the flutes on the cutter, and the principal residual stresses in the cutting and the transverse directions are oriented with respect to the helix angle. The web region is cut by the bottom of the cutter, and the principal residual stresses in the cutting and the transverse directions change depending on the tool path direction.

Aircraft structural components typically consist of multiple thin walls, as shown in Fig. 42. To predict the distortion of thin ribs and/or webs, meshing of thin walls is important for accurate results. Because thin walls can be easily modeled by a structured mesh system, a brick mesh is often used for thin-walled aircraft components. The advantages of tetrahedral meshes are that it is possible to automate initial mesh generation, remeshing, and near-surface mesh generation, which makes it possible to automate the modeling of multiple machining operations. Because automatic brick mesh generators are not available, it is not possible to do this with brick meshes. However, brick meshes provide greater accuracy, and a much smaller number of brick elements is needed to define large thin-walled airframe geometries, which reduces the computing required. A large number of tetrahedral elements are required for thin-walled airframe geometries, thereby significantly increasing the computational effort. The selection of the approach must be evaluated on a case-by-case basis depending on the component geometry, machining operations, and the distortion information required from the model.

Scientific Forming Technologies Corporation has developed a procedure to realistically model the machining process and streamline the analysis of multistep machining with the commercially available software DEFORM. A custom machining template was developed for a user to perform all the simulation steps in an automated sequence. A series of

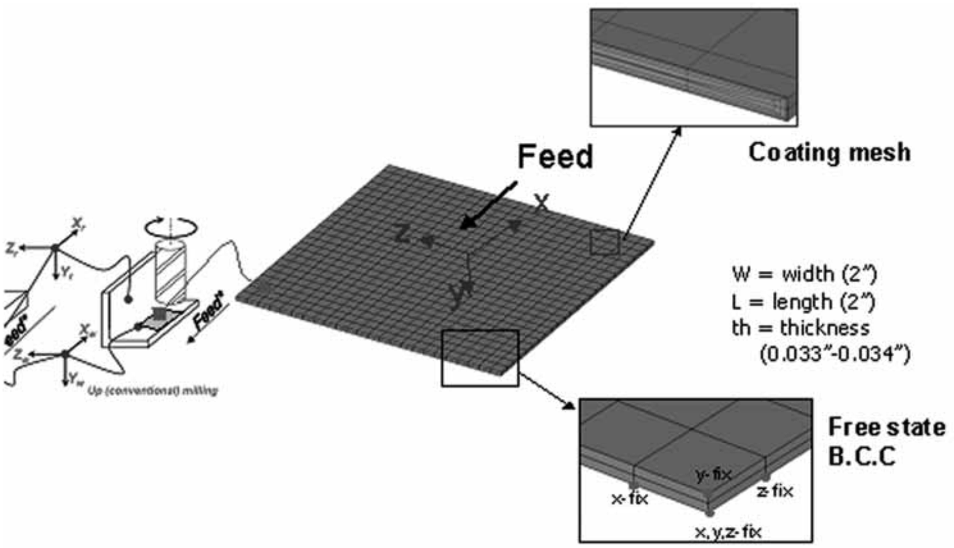

Fig. 39 Finite-element model for web coupons. bcc, body-centered cubic

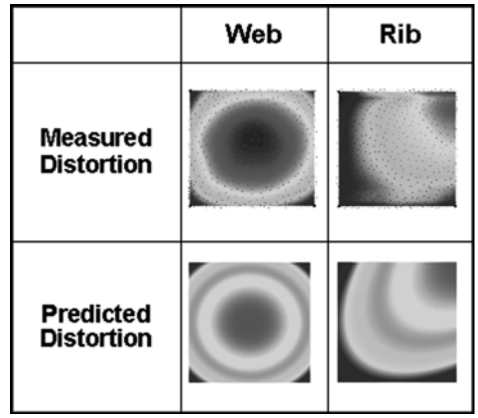

Fig. 40 Rib/web distortion. Predictions and measurements match 2 to 29%.

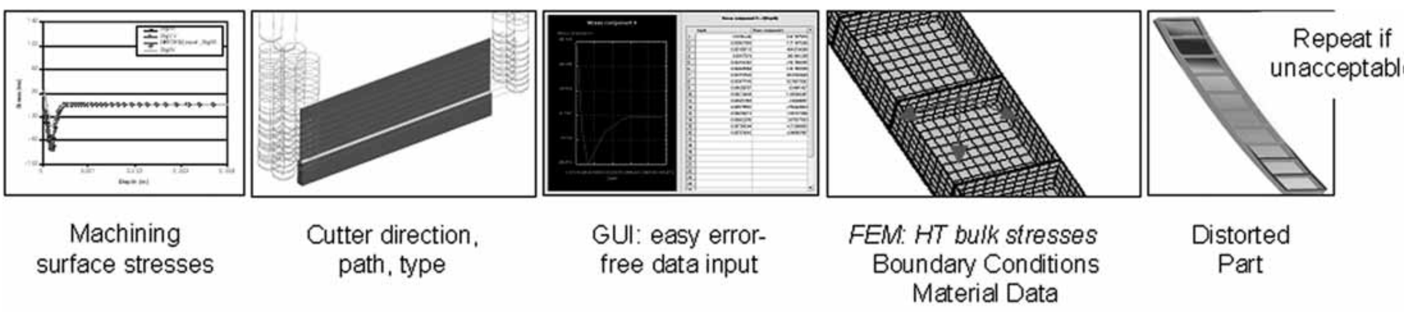

Fig. 41 Production model flow chart. GUI, graphical user interface; FEM, finite-element model; HT, heat treatment

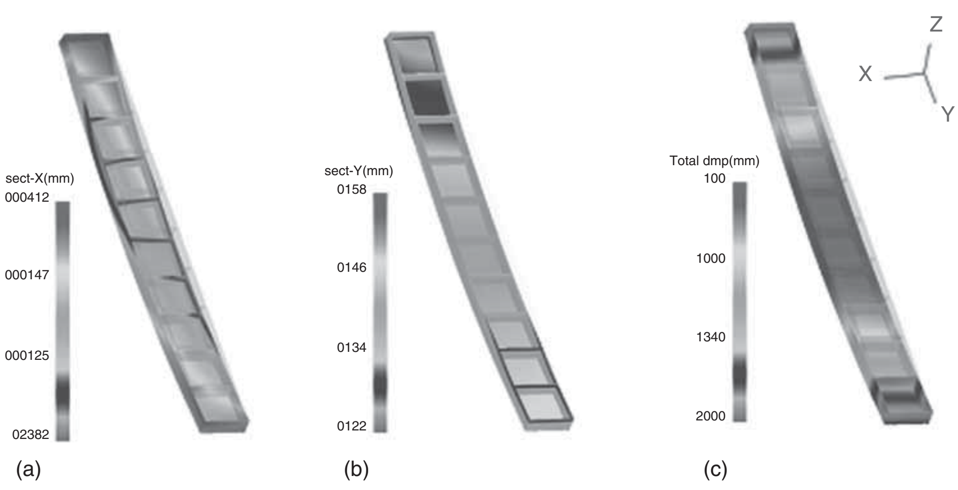

Fig. 42 Machining distortion example. (a) *x*-displacement. (b) *y*-displacement. (c) Total displacement

machining distortion simulations can be triggered from the procedure to simulate the complete process, from the heat treat shape to the final machined shape. Because machining involves the complexity of multiple passes and multiple operations, it is essential to graphically preview the relative location of the fixtures, workpiece, and machining paths prior to the analysis. This feature enables an upfront review of the entire material-removal process and ensures that all data have been input correctly. An important objective of the improved machining simulation method is to bring the modeling analysis and methods into closer alignment with the physical machining process as understood by a machining process engineer. The key challenge is to achieve the appropriate balance between improved functionality and ease of use for the resulting simulation method.

Modeling steps include Boolean operation for material removal, stress re-equilibrium under clamping condition (after material is removed), and free-state distortion (after clamps are removed). The approach starts with a residual-stress pattern and distorted heat treat shape generated using DEFORM for heat treatment process modeling. These results are then mapped onto the mesh used for machining simulation along with the geometry of the machining plan generated using CAD software and numerical control machining information. The geometry, representing the machined shape, is then meshed, clamping loads are added, and machining is carried out through element removal. A subsequent analysis is required to verify that the tooling has sufficient stiffness to withstand the rebalanced loads following machining. The machined, distorted shape is calculated following removal of clamping loads, and the entire cycle is repeated for each operation of metal removal until the finished component shape is reached. The results are presented in a format that is directly comparable to dimensional measurements. Typical results are shown in Fig. 42. For a realistic model size of a typical aircraft component, a total of approximately 150,000 elements are expected. Depending on the computer, solution method, and boundary conditions used, this model has a runtime of approximately 15 min to 3 h. Therefore, it is concluded that using DEFORM with the brick approach can be practical from the perspective of computational requirements.

Modeling Benefits

Although machining is a mature manufacturing process, the drive toward affordability continues to press established machining operations to increase metal-removal rates, increase machine utilization, and eliminate machining steps. These efforts are worthwhile because machining costs are a significant fraction of the total cost of manufacturing for aerospace forged components.

In the near-term, savings will accrue from reduced machining costs, reduced scrap, improved manufacturing lead and cycle times, reduced time to first article, and improved component performance and life during service, resulting in reduced operating costs. A more significant additional cost-savings is the ability to go to nearer-net shape forgings after this technology has been more extensively validated. Accurate prediction of distortions will enable a reduction of the material envelope needed to compensate for distortions, especially for the high-cost powder metal alloys used in rotating disks. The technology developed here is applicable to all military (United States Air Force and United States Navy) and commercial aircraft and engines.

The program is well aligned with the philosophy to achieve affordable metallic materials and processes with accelerated implementation for aerospace systems. Benefits are a reduction in acquisition costs of metallic components. Additional benefits also include potential for design of more robust components that have reduced tendency to distort during engine operation, which may affect engine clearances, efficiency, and performance.

Modeling provides a data-driven understanding of residual stress, validated commercially supported tools, and standardized modeling and measurement procedures. The MAI programs represent a major technology advance for the industry and have advanced the state of the art to a user-friendly, validated, commercially supported, and production-ready analysis tool for 3-D machining problems, which can be used to achieve significant cost-savings. Because process modeling can be used to improve both the fabrication processes and the component performance during service, it should be incorporated into the integrated design environment in the organization to achieve design for manufacturability and design for process excellence. Various design disciplines can take advantage of process models, such as service-life estimation, inspection, supplier/original equipment manufacturer (OEM) collaborations, repair, and overhaul.

The supply chain, consisting of manufacturers of aerospace components in addition to the OEMs, stands to benefit from the use of modeling. The OEMs will see a reduction in machining costs, and the forging suppliers will benefit by being able to better control the heat treatment process. Distortion problems pose the biggest challenge to new components and/or new suppliers. Modeling technology will help shorten that learning curve. Current components with distortion problems will benefit during a change of suppliers. New components will benefit right from the start. Although modeling has been demonstrated here for only selected engine and airframe materials, the model/method is pervasive and can be applied to other materials, adding to the total savings.

The methodology of this program will include the capability to evaluate the full range of process conditions for production hardware and to define process sensitivities relative to material and process variations early in the production process. This information will better define the process window. In addition, these tools could be used for evaluations when it was determined that the process window was breached.

Modeling Implementation in a Production Environment

Successful completion of the various MAI programs has permitted technology implementation on a wide variety of components. Implementation has occurred initially on new components in which process(es) could be integrated into the original design, thus reducing or eliminating additional certification costs. Subsequent production implementation to address distortion problems on existing components is based on the cost benefit balanced against any additional certification costs. Specific applications with noted cost-reduction potential include superalloy rotating components and titanium structural components. Implementation of the 2-D model is more widespread, and it has been used successfully for several production components at several OEMs. As the models become more accurate with more validation, the use and benefits will grow.

The mode and extent of use of the machining model will be somewhat user-specific, depending on the extent of validation carried out, the problem the user is trying to solve or avoid, the certainty with which the various boundary conditions and material property data during heat treatment and machining can be quantified, and so on. Here, only some general guidelines can be provided. The general implementation approach is shown in Fig. 43. The details of implementation will differ for large/small suppliers and airframe/engine components. The OEMs, forge/heat treat suppliers, and machining suppliers are involved at various stages.

This article demonstrates that finite-element modeling can be a powerful tool to predict the residual stresses developed during heat treatment processes and the distortion during machining operations. The use of commercially available software minimizes maintenance and enhancement risks. The machining template in DEFORM also provides an easy way to model the distortions developed during multioperation machining sequences. These models have been integrated with standard engineering tools and implemented within the modeling organizations at the OEMs and at their forging and/or machining suppliers.

Future Work

Future work should focus on establishing standard material characterization, measurement, and modeling methods to ensure accurate and repeatable residual-stress predictions. Additional model validation on more materials and different types of components is also needed. Suggested future work includes the following.

Roadmap. A roadmap is needed to formalize plans to address the various issues relative to residual-stress modeling, development, and rapid implementation of modeling tools that link various materials and process models and provide a known level of accuracy and uncertainty. The roadmap should identify risks and a risk mitigation plan, balancing risk, cost, payoff, and maturity. Lessons learned from engine programs should be leveraged to airframe components, recognizing the tremendous scaleup in computational requirements from 2-D engine disks to large 3-D airframe components.

Modeling and Measurement Accuracy. For the modeling results to be useful, different levels of accuracy are needed, depending on the application. The bulk residual-stress modeling and measurement accuracy required for a range of applications should be established, including manufacturing (heat treat and machining distortions), service (dimensional stability), service-life estimation (fatigue life, crack initiation and propagation), and material characterization. Various residual-stress measurement methods should be compared to develop standardized procedures and recommendations. An assessment of the accuracy and variability of the predicted and measured residual-stress profiles and their impact on manufacturing, service, and service-life estimation should be determined. Model accuracy, capability, and user-friendliness should be addressed to obtain an industrially usable tool.

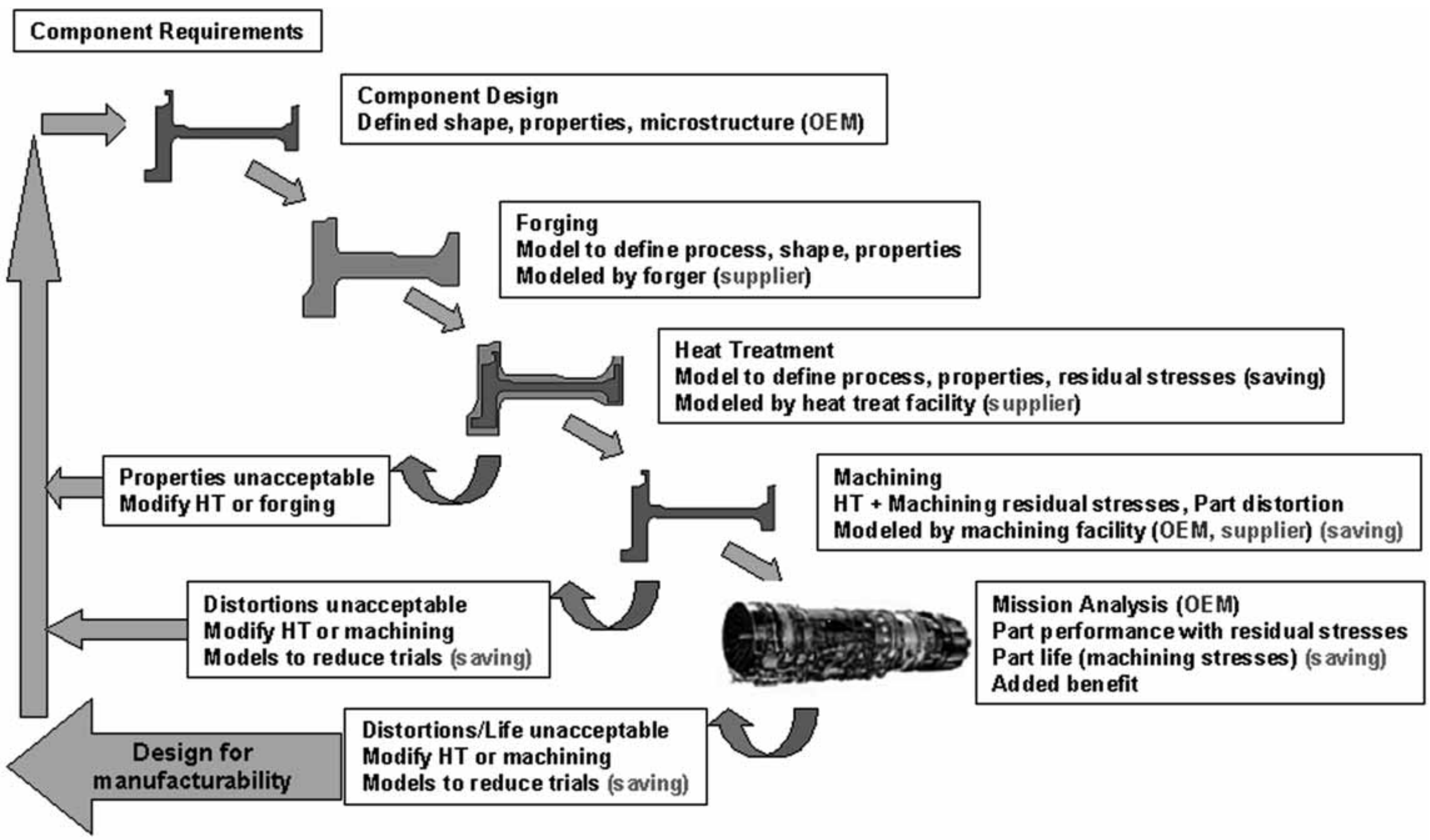

Fig. 43 General implementation approach. OEM, original equipment manufacturer; HT, heat treatment

Fig. 44 Typical aircraft engine and airframe applications

Material Data. Material constitutive properties (tensile and creep) are needed as inputs to the residual-stress models. Development of standard material test methods (on-cooling tensile and creep/stress relaxation) and an industry-wide data set for commonly used alloys will reduce uncertainty and improve modeling accuracy. These data sets could more thoroughly cover the full range of temperatures, strain rates, and microstructural conditions than would be economically feasible for a single company. Modeling enhancements are also needed to incorporate these data into the model in a standardized way and to develop a physics-based model, which includes microstructure evolution and deformation mechanisms to describe material behavior during heat treatment. Effects of evolving microstructural features and crystallographic texture on elevated-temperature mechanical properties should be evaluated. If these are significant, a testing plan to capture these effects should be developed. The methodology should also include aluminum airframe and nickel-base engine disk materials.

Validation. Residual-stress predictions require further validation to support their quantitative application to various applications. Validation is needed on subscale and full-scale components in a production environment, streamlining and integration of commercial codes for user-friendly industrial implementation, and developing industry guidelines for model usage. Use cases that codify the methodology and describe the problem-solving steps have been used successfully in prior programs to demonstrate the modeling framework. Standard benchmark use cases should be defined to design a heat treatment and machining process to better balance properties and distortions and to identify optimal parameters. This involves the generation of experimental data under controlled and production conditions and extensive model validation followed by implementation on production hardware (Fig. 44). This effort will allow comparison and transfer of residual-stress predictions seamlessly through the supply chain, including mills, forge suppliers, OEMs, and machining suppliers.

Modeling Sensitivity Studies. Traditionally, engineering analysis is performed for nominal conditions. The design must account for various sources of uncertainty inherent in materials behavior, manufacturing processes, models, and so on to arrive at a robust control strategy to ensure minimal variability in the component characteristics. The error in residual-stress predictions can be estimated by a Monte Carlo analysis driven by probability density functions that describe the uncertainty in inputs (e.g., heat-transfer coefficients and material properties). An error propagation analysis should be used to quantify the compounding of errors as the analysis progresses through various steps.

This will establish confidence limits on the modeling predictions and experimental measurements.

A sensitivity study is recommended to establish which inputs most strongly impact the modeling outputs of interest. Variations in the critical inputs should be quantified to assess the accuracy of the modeling outputs. Efforts can then be focused on reducing the variability in component distortion by studying the most critical steps. The sensitivity analysis can also potentially define the resolution needed in the input material property data.

Qualitative analysis is the capability to predict the trend under different processing conditions. Engineers can use this to carry out many "what-if" studies without the need to rely on expensive experiments. Quantitative analysis is the capability to accurately predict the component behavior. This requires an accurate modeling algorithm and input parameters/data, including both the boundary conditions and material properties.

Industry Standards. Residual-stress modeling and measurement techniques and the procedures to generate the various modeling inputs lack a standardized approach. An industry standard must be established that can be used throughout the supply chain (mills, component producers, and OEMs) to enable integrated design, material, and processing technology efforts. As a "best practice," the analysis and experimental methods should include metrics, red flags, and/or guidelines to permit a quantitative assessment of the adequacy of each analysis and measurement. It should also include instructions about the range of applicability of the associated methods. Standards for modeling and measurement procedures, material data, and boundary condition inputs should be prepared. The goal would be to develop standard methods in the form of an Aerospace Material Specification. Developed best practices (input data, simulation, postprocessing) should be aimed at producing consistent results, independent of the user, with acceptable accuracy.

ACKNOWLEDGMENTS

The authors would like to acknowledge the contributions of the team members in the various Metals Affordability Initiative Programs: Keith Young and James Castle (Boeing); B.K. Chun, W.T. Wu, M. Knezevic, and J.Y. Oh (Scientific Forming Technologies Corp.); Michael Glavicic and Robert Ress (Rolls-Royce); and Jeff Simmons (Air Force Research Laboratory).

REFERENCES

1. P.L.B. Oxley, *The Mechanics of Machining: An Analytical Approach to Assessing Machinability,* E. Horwood, Halsted Press, New York, 1989, p 242
2. J. Gayda, "The Effect of Heat Treatment on Residual Stress and Machining Distortions in Advanced Nickel-Based Disk Alloys," NASA/TM-2001-210717
3. W.-T. Wu, G. Li, J. Tang, S. Srivatsa, R. Shankar, R. Wallis, P. Ramasundaram, and J. Gayda, "A Process Modeling System for Heat Treatment of High Temperature Structural Materials," Final report, USAF Contract F33615-95-C-5238, June 2001
4. J.-C. Su, "Residual Stress Modeling in Machining Processes," Ph.D. thesis, Georgia Institute of Technology, 2006

SELECTED REFERENCES

- T.G. Byrer, Ed., *Forging Handbook,* Forging Industry Association, American Society for Metals, 1985
- D. Dye, K.T. Conlon, and R.C. Reed, Characterization and Modeling of Quenching-Induced Residual Stresses in the Nickel-Based Superalloy IN718, *Metall. Mater. Trans. A,* Vol 35, June 2004, p 1703
- T.P. Gabb, J. Telesman, P.T. Kantzos, and K. O'Connor, "Characterization of the Temperature Capabilities of Advanced Disk Alloy ME3," NASA/TM 2002-211796
- D.L. McDowell and G.J. Moyar, A More Realistic Model of Nonlinear Material Response: Application to Elastic-Plastic Rolling Contact, *Proceedings of the Second International Symposium on Contact Mechanics and Wear of Rail/Wheel Systems* (Kingston, RI), 1986
- T. Reti, Z. Fried, and I. Felde, Computer Simulation of Steel Quenching Process Using a Multi-Phase Transformation Model, *Comput. Mater. Sci.,* Vol 22, 2001, p 261–278
- M.A. Rist, S. Tin, B.A. Roder, J.A. James, and M.R. Daymond, Residual Stresses in a Quenched Superalloy Turbine Disc: Measurements and Modeling, *Metall. Mater. Trans. A,* Vol 37, Feb 2006, p 459
- D. Rondeau, "The Effects of Part Orientation and Fluid Flow on Heat Transfer Around a Cylinder," M.S. thesis, Worcester Polytechnic Institute, 2004
- G. Shen and D. Furrer, Manufacturing of Aerospace Forgings, *J. Mater. Proc. Technol.,* Vol 98, 2000, p 189–195
- "Standard Test Method for Determining Residual Stresses by the Hole-Drilling Strain-Gage Method," E 837-08, ASTM
- "Standard Test Methods for Stress Relaxation for Materials and Structures," E 328-02 (Reapproved 2008), ASTM
- P.J. Withers and H.K.D.H. Bhadeshia, Overview: Residual Stress Part 1—Measurement Techniques, *Mater. Sci. Technol.,* Vol 17, April 2001, p 355
- P.J. Withers and H.K.D.H. Bhadeshia, Overview: Residual Stress Part 2—Nature and Origins, *Mater. Sci. Technol.,* Vol 17, April 2001, p 366